SEISMIC SEQUENCE STRATIGRAPHY OF PLIOCENE-PLEISTOCENE TURBIDITE SYSTEMS, SHIP SHOAL SOUTH ADDITION, NORTHWESTERN GULF OF MEXICO

A Thesis

by

BOOYONG KIM

Submitted to the Office of Graduate Studies of
Texas A&M University
in partial fulfillment of the requirements for the degree of

MASTER OF SCIENCE

August 2002

Major Subject: Geophysics

SEISMIC SEQUENCE STRATIGRAPHY OF PLIOCENE-PLEISTOCENE TURBIDITE SYSTEMS, SHIP SHOAL SOUTH ADDITION, NORTHWESTERN GULF OF MEXICO

A Thesis

by

BOOYONG KIM

Submitted to Texas A&M University
in partial fulfillment of the requirements
for the degree of

MASTER OF SCIENCE

Approved as to style and content by:

Joel S. Watkins (Chair of Committee)	Luc T. Ikelle (Member)
W. John Lee (Member)	Andrew W. Hajash (Head of Department)

August 2002

Major Subject: Geophysics

ABSTRACT

Seismic Sequence Stratigraphy of Pliocene-Pleistocene Turbidite Systems,
Ship Shoal South Addition, Northwestern Gulf of Mexico. (August 2002)
Booyong Kim, B.S., Kyungpook National University
Chair of Advisory Committee: Dr. Joel S. Watkins

During the Late Pliocene to Middle Pleistocene Ages, sediments of the study area were deposited in the intra-slope salt withdrawal basin where sand-prone sediments deposited as turbidite lobes and channel fills are the main reservoirs of the Northern Gulf of Mexico. The main purpose of this study was to identify and characterize these sand-prone sediments. Sequence stratigraphic analysis of well logs, biostratigraphic data, and 3-D seismic data provided a chronostratigraphic framework of the study area, within which seismic facies analysis was carried out. Each sequence was subdivided into separate seismic bodies characterized by specific amplitude, coherence of reflectors, and shape of reflectors. The descriptions of each seismic facies combined with well logs were compared with turbidite facies models to infer their geological information. Five turbidite elements were identified: depositional channel fills and overbank deposits, erosional channel fills, turbidite lobes, mud turbidite fills and sheets and hemipelagic and pelagic drapes. Depositional channel fills are usually deposited in lower parts of interpreted sequences, surrounded by shale-prone overbank deposits. The lateral variation of these turbidite elements was revealed by horizon slices, in which depositional channels are generally trending NE-SW or NNE-SSW with elongated sinuous forms. Well logs indicate that depositional channel fills usually consist of bell or cylinder type sand-prone sediments. Turbidite lobe was found only in the 1.1-0.8 Ma sequence, in which it laps out onto the underlying sequence boundary and shows high-amplitude and a high-coherence of mound shape. This facies is interpreted as sand-prone, but wells available penetrated only the marginal parts of this facies and showed poor reservoir qualities. Horizon slices could partly reveal its lapout boundary due to the

limitation of vertical seismic resolution. Mud turbidite fills and sheets are the most dominant turbidite facies, which usually occurred in the upper parts of sequences and overlain by hemipelagic and pelagic drapes. Hemipelagic and pelagic drapes were deposited very widely, wrapping down the previous topography with consistent thickness throughout the basin. Erosional channel was observed only in the 0.8-0.7 Ma sequence where it cut into the underlying sequence and was filled by shale-prone sediments. Depositional channel fills and turbidite lobes are the main reservoir facies in the study area. Seismic facies analysis using vertical seismic sections and horizon slices combined with lithology data made it possible to identify and systematically describe these sand prone turbidite elements in intra-slope salt withdrawal basin.

DEDICATION

To my wife, Myungok Kim, for her love, support, and patience.

ACKNOWLEDGMENTS

I sincerely acknowledge:

Dr. Joel S. Watkins, the chairman of my advisory committee, for his helpful advice and comments throughout my studies at Texas A&M and for the review of this thesis.

Dr. Luc T. Ikelle and Dr. John Lee for filling out the advisory committee and for their helpful advice and comments for this project.

Dr. Steven L. Dorobek for his excellent courses in basin architecture and stratigraphy.

Korea National Oil Corporation for providing financial support as I pursued a master's degree at Texas A&M University.

Dr. Inchang Rhyu, German Molina and Changsu Ryu for helpful discussions and suggestions throughout the development of this project.

My wife for her support and assistance throughout my study.

TABLE OF CONTENTS

Page

LIST OF FIGURES

Figure Page

Figure Page

Figure Page

LIST OF TABLES

1. INTRODUCTION

Numerous intraslope basins developed by salt and fault evolutions can characterize the slope of the Gulf of Mexico. These basins are severely deformed by salt upwelling and fault deformations and are usually filled by Neogene turbidite sediments. This Neogene turbidite system commonly contains sand-prone turbidite sediment deposited as lobes or channels. These sand prone turbidite deposits are the main reservoirs in the northern Gulf of Mexico (Weimer et al., 1998 and Varnai, 1998). Many attempts to understand the spatial and temporal distribution of these sand prone turbidite deposits in intraslope basins have been made because of their significance in hydrocarbon exploration activities in the Northern Gulf of Mexico.

This study focuses on describing and characterizing the Neogene turbidite strata deposited in an intra-slope basin in the northern Gulf of Mexico. Sequence stratigraphic analysis was carried out using high-resolution three-dimensional seismic data. The interpretation of well logs and biostratigraphic data provide key information to locate sequence boundaries and condensed sections in the study area where erosional surfaces or lap-out patterns are not commonly observed from the seismic data. The integrated results of sequence analysis from different kinds of data sources were especially useful to build a reasonable chronostratigraphic framework in the study area. Seismic facies analysis with high-resolution, 3-dimensional seismic data within a time-constrained framework clearly showed the depositions of channel or lobe-shaped turbidite sediments. A series of horizon slices created by sequence boundaries or condensed sections successfully revealed the variation of these sand-prone turbidite facies in space and time.

This thesis follows the style and format of the American Association of Petroleum Geologists Bulletin.

1.1 Objectives

The objectives of this study are (1) to describe the structural patterns of the Pliocene and Pleistocene turbidite systems with high-resolution 3-D seismic data, (2) to build a chronostratigraphic framework of Late Pliocene and Pleistocene deposits in a sloped mini-basin with sequence stratigraphic concepts, (3) to carry out seismic facies analysis within a chronostratigraphic framework, and (4) to integrate seismic facies with well data and biostratigraphic information to infer paleo-depositional environments and lithofacies.

1.2 Study Area

The study area is located over the near the present shelf edge and the upper slope in offshore Louisiana, Northern Gulf of Mexico (Figure 1). It includes the southern part of Ship Shoal South Addition, the eastern part of Ewing Bank, and the northern edges of Green Canyon covering the area of 152 square kilometers (the red-colored rectangle in Figure 1). The present shelf-slope break is located in the southern part of the study area where an intraslope mini-basin is buried by prograding shelf sediments.

1.3 Data Base

Sub-regional 3-D seismic data and six well data were used for this study. 3-D seismic data used for this study are the subset of the 300 square kilometers of migrated 3-D seismic data set acquired by BHP Petroleum. The seismic data were acquired in an east-west direction. The line and trace intervals are 65 ft and 41 ft respectively. Well data available include wireline logs, biostratigraphic data, time-depth information, and well cutting descriptions (Table 1), the qualities of which are variable from good to poor. Biostratigraphic data consist of benthic foraminifer datum, calcareous nannoplancton

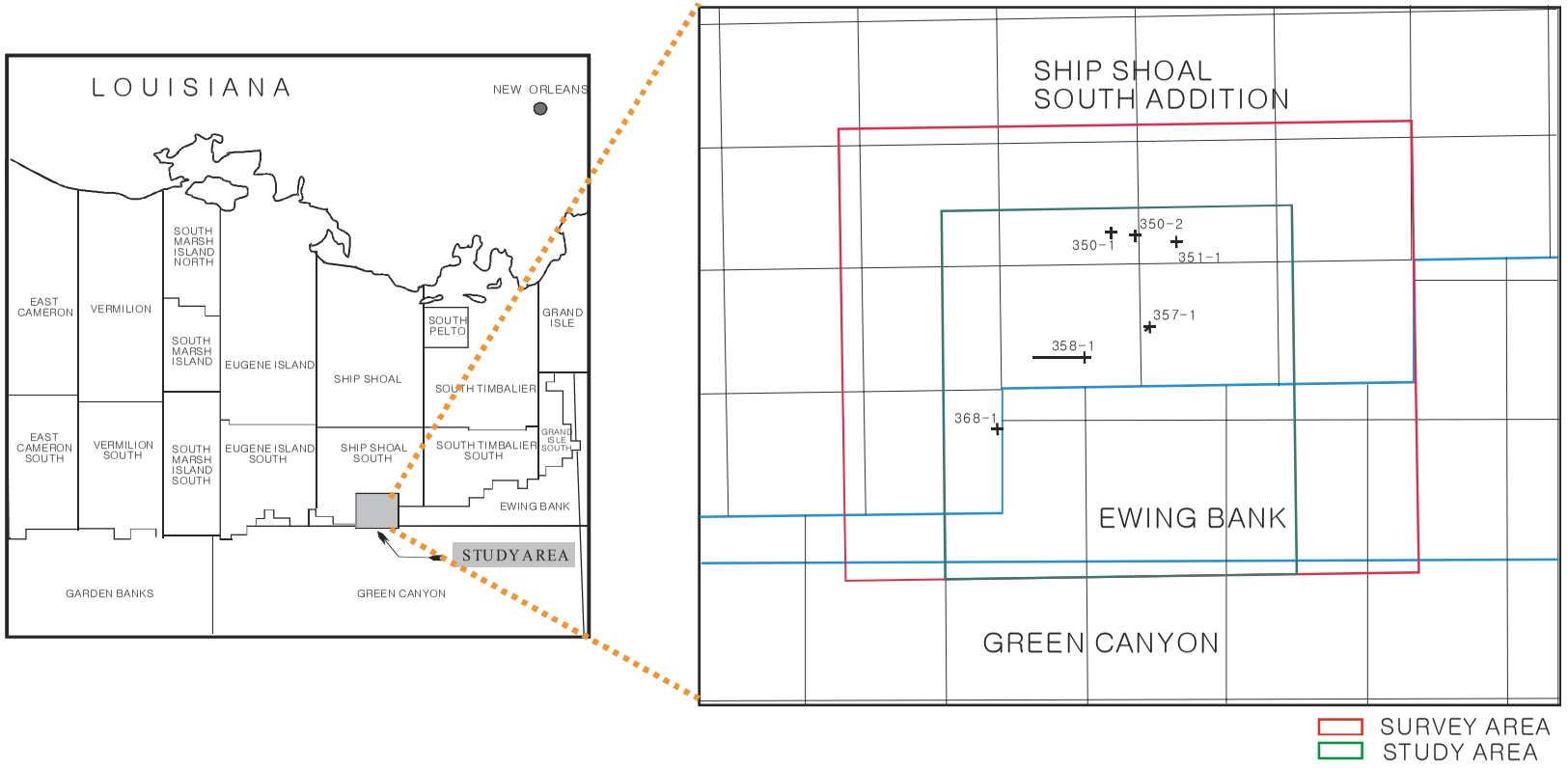

Figure 1. Location of study area and well locations.

Table 1. Well database.

Well	*Gamma Ray Log*	*SP Log*	*Resistivity Log*	*Neutron-Density Log*	*Sonic Log*	*Calcareous Nanno-Planktons Datum*	*Benthic Foraminifer Datum*	*Fossil Abundance and diversity curves*	*Time-depth information*
350-1	X	X	X		X	X	X	X	X
350-2	X	X	X		X	X	X	X	X
351-1	X	X	X	X	X		X		
357-3	X	X	X	X	X		X		
358-1	X	X	X	X	X	X	X		
368-1	X	X	X		X		X		X

datum, and fossil abundance and diversity curves. Time-depth information was obtained from the Website of the Minerals Management Service, Gulf of Mexico OCS Region. Geographics, well log interpretation software, was used to digitize and interpret well data. LandMark 3-D seismic interpretation package and StratWorks were exclusively used for interactive 3-D seismic data interpretation, and well-to-seismic correlation.

1.4 Methodology

This study was performed according to the following procedures:

The first step was structural interpretation, for which the top salt and equivalent salt surfaces were mapped throughout the study area and a time-structural map was created. Faults were also interpreted from both the vertical seismic sections and horizontal time slices. The structure of the study area can be characterized by severe deformation caused by salt and fault evolutions. However, 3-D seismic data provide a high-resolution subsurface image, with which high-quality fault and salt mapping was possible.

The second step was to build a sequence-stratigraphic framework for the study area. The general procedure of sequence stratigraphic analysis was adapted from Vail and Wornardt (1991). Key surfaces including condensed sections and sequence boundaries were identified from fossil abundance data, paleo-top information, and well logs. All sequence boundaries and condensed sections were correlated with a global cycle chart to date and tied with seismic data using time-depth information. Each reflector correlated with a sequence boundary was interpreted throughout the study area, and the time-structural maps and isochron maps were generated for the interpreted sequences.

The final step was seismic facies analysis, which was performed within the chronostratigraphic framework provided by sequence stratigraphic analysis. Seismic parameters including reflection configuration, amplitude, and coherency were examined from the vertical seismic sections to describe seismic parameter variations that may be

caused by geologic changes within seismic sequences and systems tracts. Horizon slices created by 3-D seismic volume flattened by sequence boundaries or condensed sections were used to describe the lateral variations of the seismic facies. Seismic facies combined with well logs were correlated with facies models and interpreted into geological facies associations or turbidite elements.

2. STRUCTURAL INTERPRETATION

The study area can be characterized by highly complex structural patterns consisting of allochthonous salt bodies, extensional faults and contraction folds and faults. The deformations of salts and associated faults are closely related with the sedimentations in the study area. Most faults are related to the deformation of the allochthonous salt bodies. During the Cenozoic Ages, the evolution of the basin was dominated by the influx of large clastic sediments, which caused the basinward evacuation of autochthonous Jurassic salt (McBride, 1998). The allochthonous salt bodies in the study area were deformed again as sediment prograded and generated a small-scale intraslope salt-withdrawal basin.

Stratigraphic interpretation without understanding of salt and fault deformations may result in significant miscorrelations in this area because of its structural complexity. Thus, the detailed interpretation of salt and faults is an essential step prior to any stratigraphic interpretations in the Gulf of Mexico (Weimer et al., 1998). Faults were interpreted using high-resolution three-dimensional seismic data, which made it possible to map and correlate the fault systems in this highly deformed area. The top surface of scattered salt bodies and their equivalent welded surfaces were also interpreted using high-resolution 3-D seismic data, which made it possible to understand the geometry and distribution of salt bodies. The geometry of the salt withdrawal basin of the study area was very also well explained by the salt interpretation.

2.1 Fault Interpretation

Fault activities are closely related with salt deformation in the northern Gulf of Mexico, where extensional faults, contractional faults and strike-slip faults developed as effects of salt mobilization. This diversity is caused by the characteristics of the salt deformation driven by sediment loading (Jackson and Galloway, 1984; Worrall and

Snelson, 1989; Wu et al., 1990; Diegel et al., 1995; Peel et al., 1995; Rowan, 1977). As the sedimentary overburden increases, gravity-driven deformation occurs resulting in listric normal faults dipping to basinward. These fault surfaces usually attach onto the salt detachment surfaces. Extensional faults characterize the landward and middle part of the linked systems, contraction usually occurs near the basinward limits, and strike-slip deformation may connect these two domains (Rowan, 1997).

In the study area, normal faults commonly developed in the north, east and west boundaries of the mini-basin. These extensional faults are developed above the shallow salt sheets forming a curve linear trend in plan view (Figure 2 and 3). In vertical section these faults show normal movement. These faults developed on top of salt highs located in eastern and western boundaries of this basin and trending generally in NNE-SSW directions. These fault systems consist of numerous fault surfaces (Figure 3). Thus, only the limited number of distinguished fault surfaces could be correlated from this study using vertical seismic sections and horizontal time slices. In Figure 3, the time slice cut at 1260 msec, we can see that instantaneous frequency data provide a better picture for fault interpretation than normal amplitude data, so several instantaneous frequency data were used to find out general trends of faults.

To the south, two types of reverse faults trending east to west and dipping landward developed (Figure 4). These are interpreted as break-thrust fault and tow-thrust fault (after Rowan, 1997). Break-thrust faults developed in the southern part of the study area bounding the basin (Figure 4) dipping to the north. Break-thrust fault are usually symmetric, steep, reverse faults dipping both landward and basinward, cutting the salt-cored fold (Rowan et al., 1999). However, the break-thrust faults interpreted in this study developed around salt-cored folds dipping only landward (Figure 4, 5 and 6). The maximum fault throws are observed in the southeastern part of the basin and decreased significantly to the west (Figure 4 and 6). It is believed that these faults were activated in the late stage of folding and continued until about 0.6 Ma. After 0.6 Ma the fault activities decreased because of salt evacuation from the central part of the basin. The other contractional fault, a toe-thrust fault, shows a pattern in plan view similar to

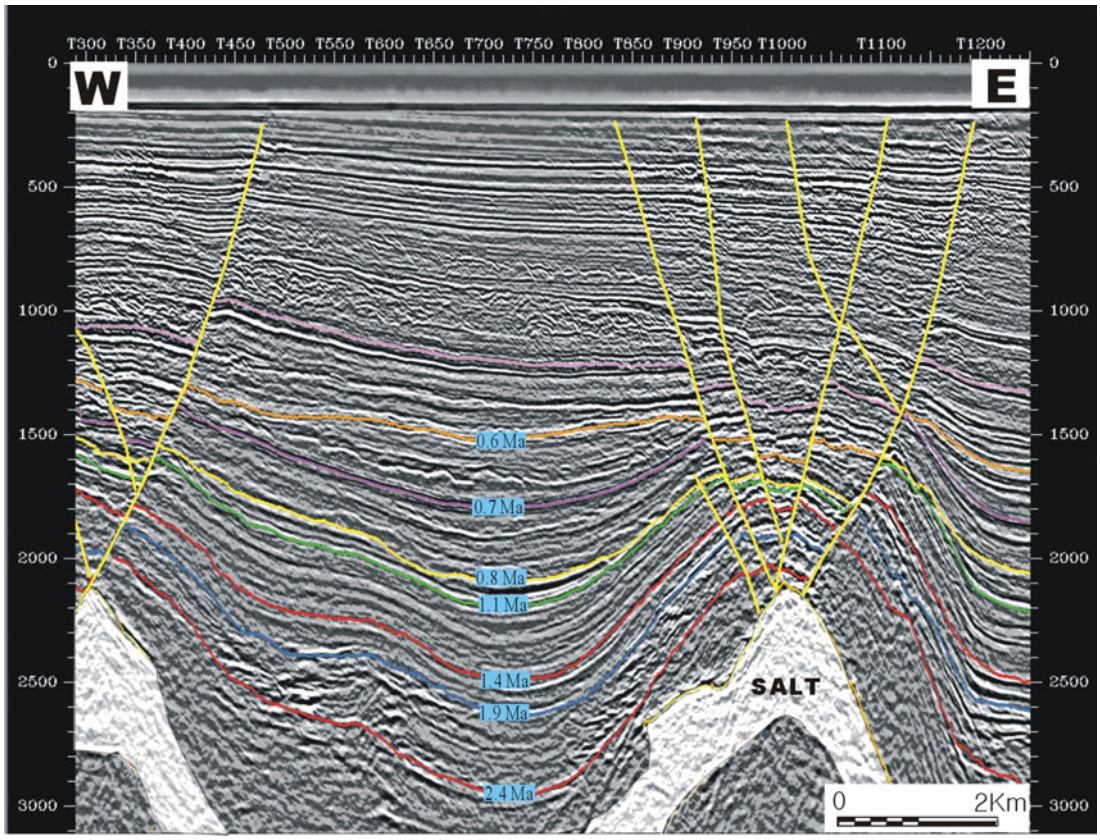

Figure 2. Seismic section showing extensional faults developed on tops of salt bodies. See Figure 4 for the location of section.

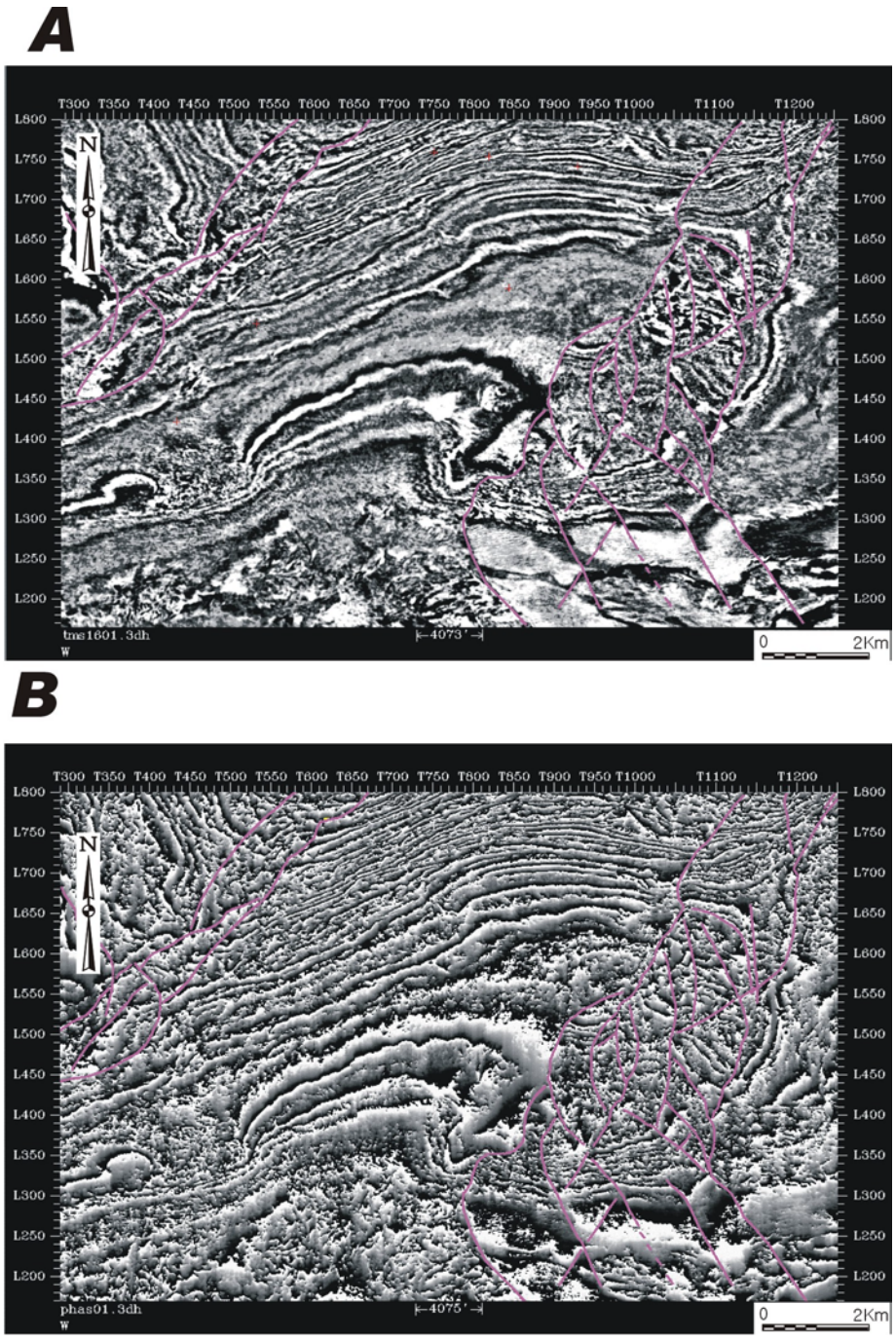

Figure 3. Time slice at 1260 msec showing extensional faults in plan view. A: amplitude display B: instantaneous frequency display.

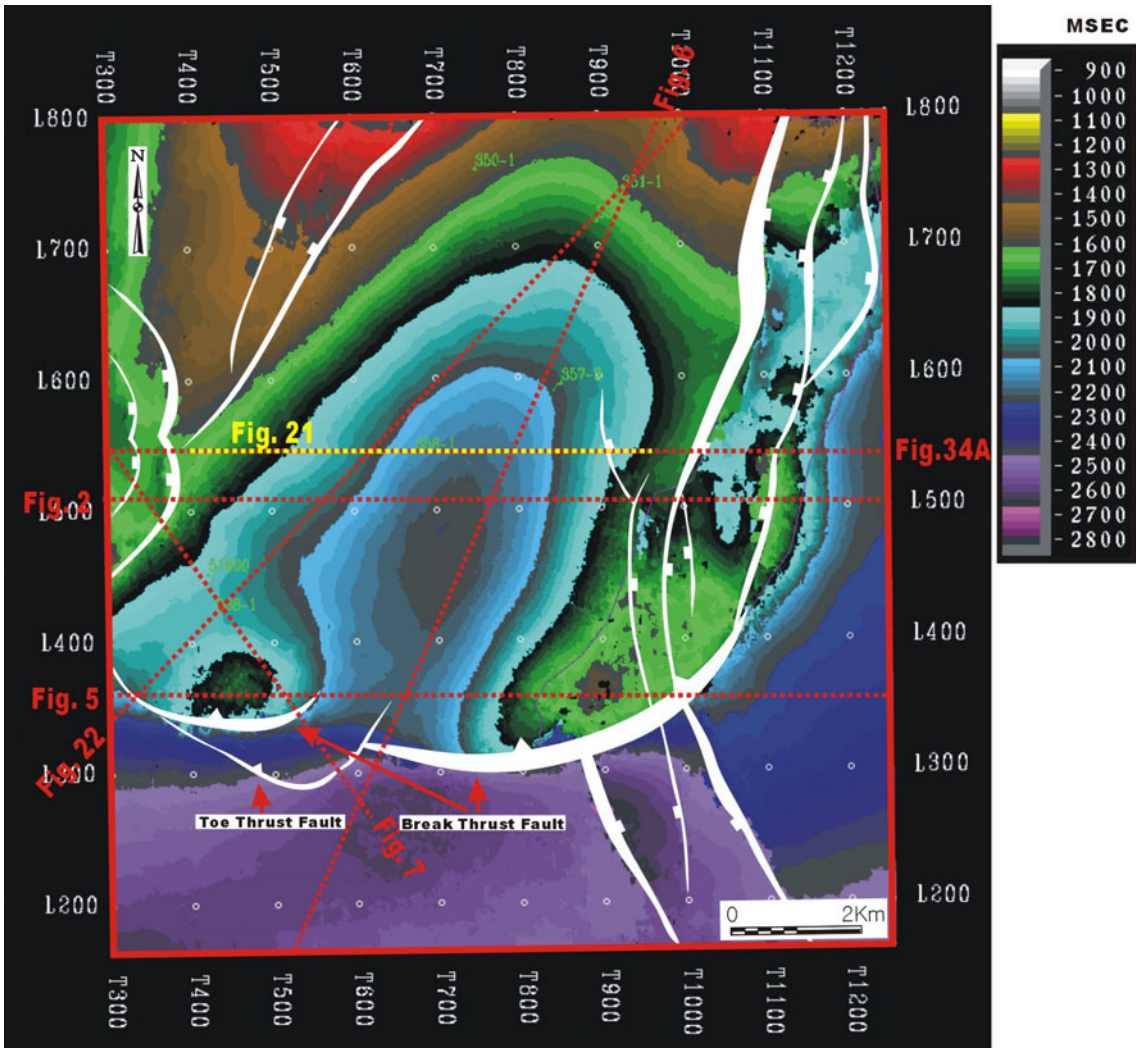

Figure 4. Time structure map of sequence boundary 1.1 Ma showing general fault patterns in the study area.

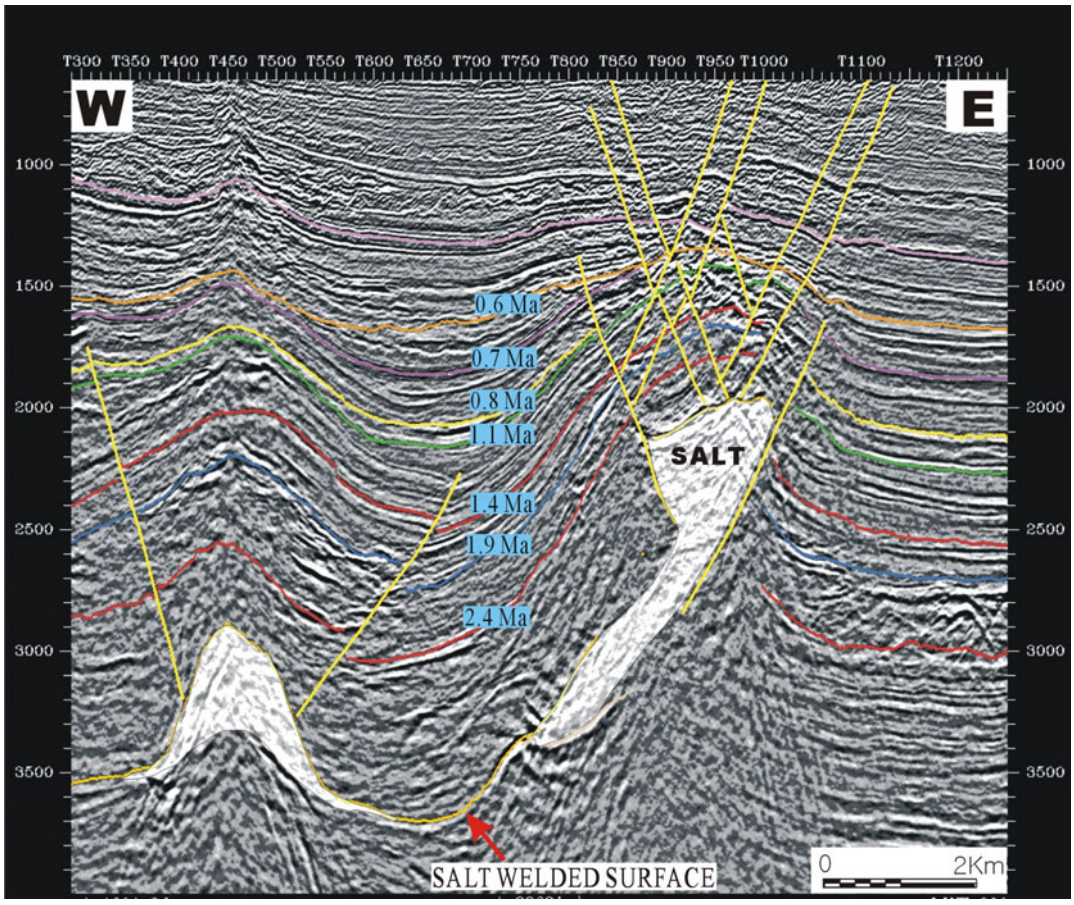

Figure 5. Depositional strike-oriented seismic section showing break-thrust faults developed by salt upwelling. See Figure 4 for the location of seismic section.

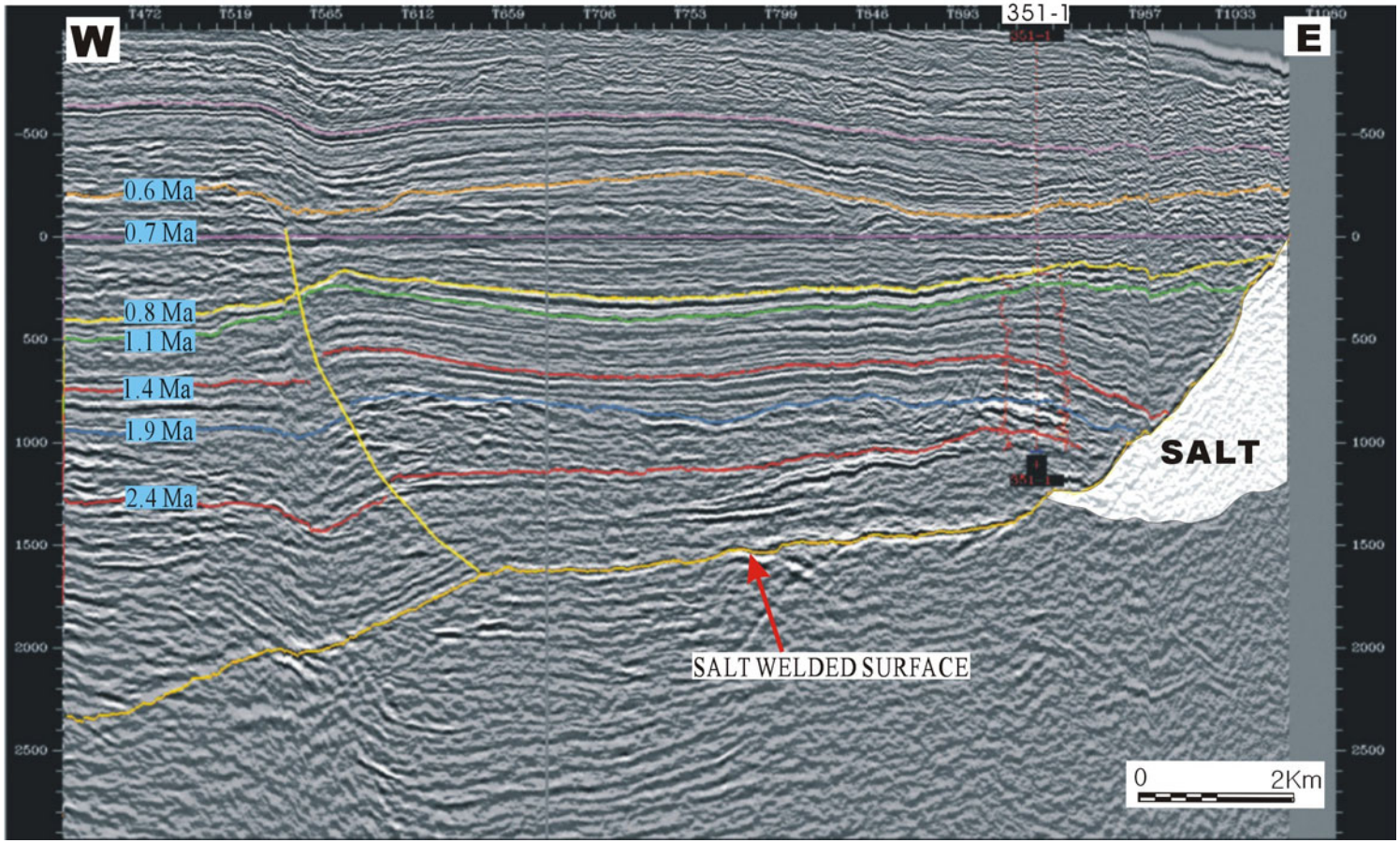

Figure 6. NE-SW trending seismic section flattened by 0.7 Ma sequence boundary. Notice significant thickening of sediment against salt body in 1.4-1.1 Ma sequence. See Figure 4 for location of seismic section.

the break-thrust fault's (Figure 4). This fault is also a reverse fault, dipping landward, and mainly developed by sediment translation deposited on the allochthonous salt body (Figure 7). This fault usually develops at the toes of the allochthonous salt body or its evacuated equivalents (Rowan et al., 1999). Only one toe thrust fault was mapped in the southwestern part of the study area where it is dipping northwest and attached onto the salt welded surface (Figure 4 and 7). It developed without salt-cored folds and is differentiated by less steepness of the fault surface from the break-thrust faults.

2.2 Salt Interpretation

The top salt surface is characterized as continuous, strong, positive-amplitude reflectors because salt has a much higher velocity than other clastic sediments in the Gulf of Mexico. Therefore, these reflectors can be easily defined from the most of the study area; but where salt bodies are located under severely faulted structures, they are not easily interpreted, even with the high-resolution 3-D seismic data. The geometry of the salt-withdrawal basin of the study area was very well explained from the salt interpretation (Figure 8). Shallow salt bodies are distributed in the north, east and west parts of the basin where its depth in two-way time ranges from 1.5 to 2.5 seconds. In the central part of the basin, most of the salt was evacuated, probably at around 0.6 Ma, as indicated by the series of isochron maps generated with interpreted sequence boundaries. Sequences below the 0.6 Ma sequence boundary show that the depocenters are located in the central part of the basin. However, the depocenters of the sequence above the 0.6 Ma sequence boundary moved to the north; that is caused by the growth fault dipping basinward and by salt deformation (Figure 6). The salt-welded surface is extended to the south and might be connected to the deep salt body in the downdip area by a ramp-type welded surface.

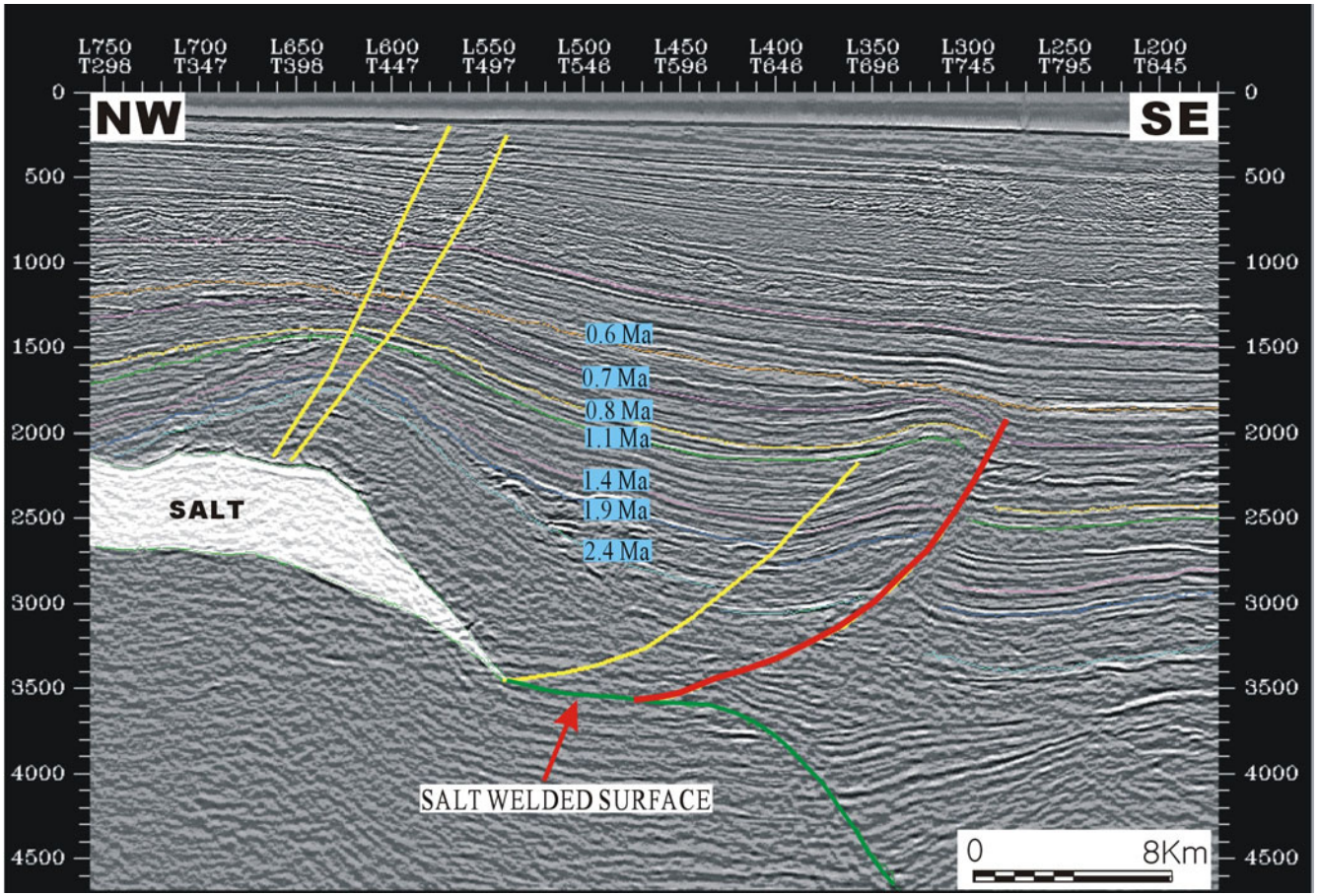

Figure 7. NW-SE trending seismic section showing extensional faults on top of the salt (yellow) and toe-thrust faults dying out onto the salt welded surface (red). See Figure 4 for the location of seismic section.

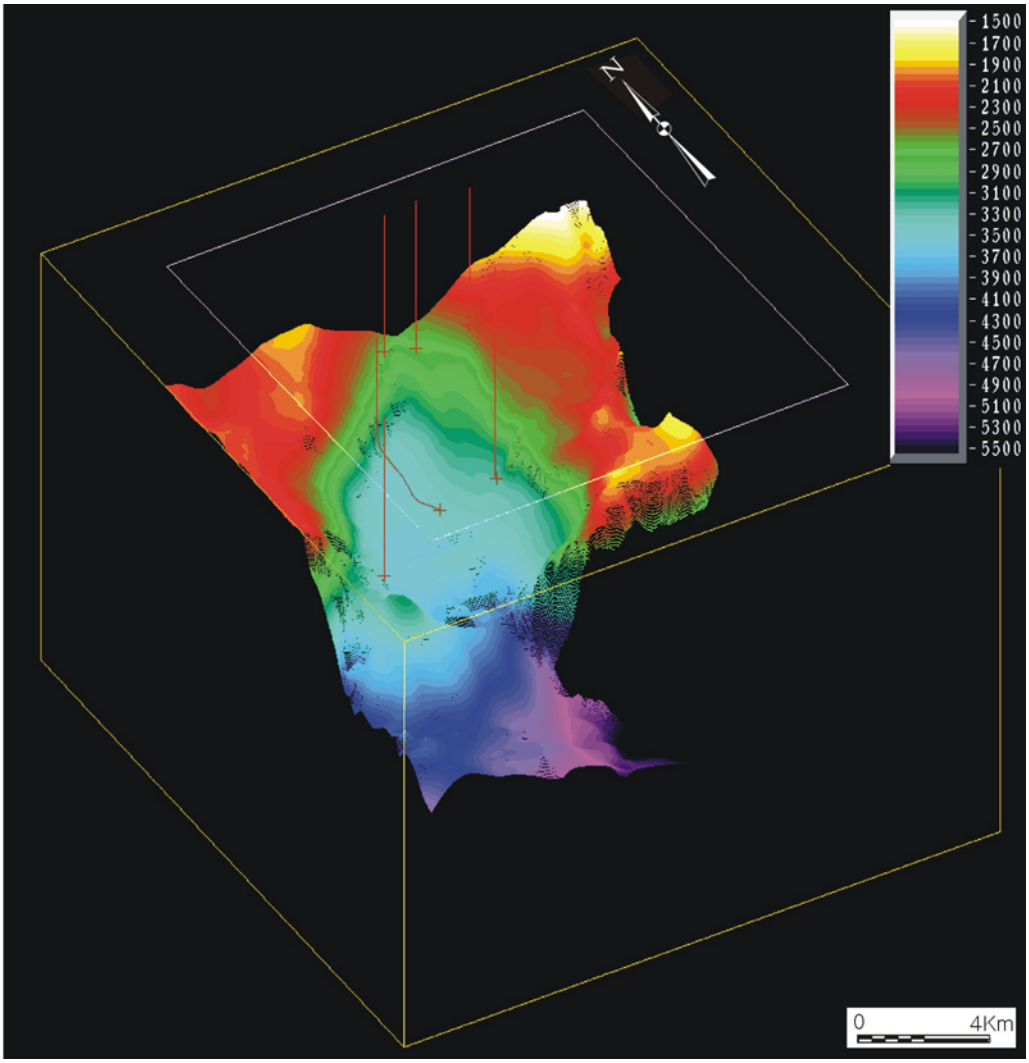

Figure 8. 3-D view of the time structure of the top of salt surfaces and their equivalent salt welded surface. Yellow to red colors indicate salt high areas and cyan to blue colors indicate salt-evacuated area.

2.3 Basin Geometry and Its Evolution

The study area lies in the outer shelf, shelf-slope break and the most upper slope of the unstable progradational shelf-slope system, offshore Louisiana (Figure 9). During the Late Pliocene to Early Pleistocene Ages, however, it is interpreted that it was located in the middle to upper slope, where sediments were deposited in a deepwater setting intraslope basin formed by salt-withdrawal activities. According to Geitgey's work (1988), the paleo-shelf break of 0.6 Ma was located about 10 miles north of the study area. In the northern Gulf of Mexico, salt mobilization and associated growth faults supplied a considerable amount of accommodation space and severely modified sedimentation patterns (Simmons, et al., 1996). Depocenters were usually formed by salt mobilization and displacement of pre- and syn-depositional sediment (Watkins, et al., 1996). Growth faulting was active along the landward boundary of the salt-withdrawal basin, which provided additional accommodation space and enlarged these depocenters (Watkins, et al., 1996).

This basin is an elliptical shape, elongated to the NNE-SSW direction (Figure 8). The north, east and west sides of the basin are bounded by extensional faults and topographic highs caused by salt upwellings. Downdip margins are bordered by salt-cored folds and reverse faults. These topographic highs caused by salt deformation functioned as partial downdip barriers to sedimentation, trapping more sediment within the basin. The faulting and salt upwelling interactively affected the sedimentation pattern in this area, which can be easily explained by the series of isochron maps generated by the interpreted sequence boundaries (Figure 10). From 2.4 Ma to 0.6 Ma, sedimentation was mostly controlled by salt withdrawal and depocenters located in the central part of the basin where salt evacuation dominantly occurred. After 0.6 Ma, salt evacuation was ceased from the central part of the basin and no further significant accommodation space was provided by the salt deformation. Sedimentation was also controlled by the fault activities. In the northern part of the basin, another depocenter was created during 1.4-1.1 Ma sequence where sediments show significant expansion against the basinward-

dipping growth fault (Figure 6 and 10). According to Weimer et al. (1998), the study area was under a lower bathyal environment (biofacies Zone 5) during the Late Pliocene to Early Pleistocene periods. After 0.6 Ma, it can be interpreted from isochron maps and the results of seismic facies analysis that salt evacuation was ceased from the central part of the basin and shelf/slope break prograded near the study area, so that bypass, slide and slump sediments are commonly recognized in the younger sequences.

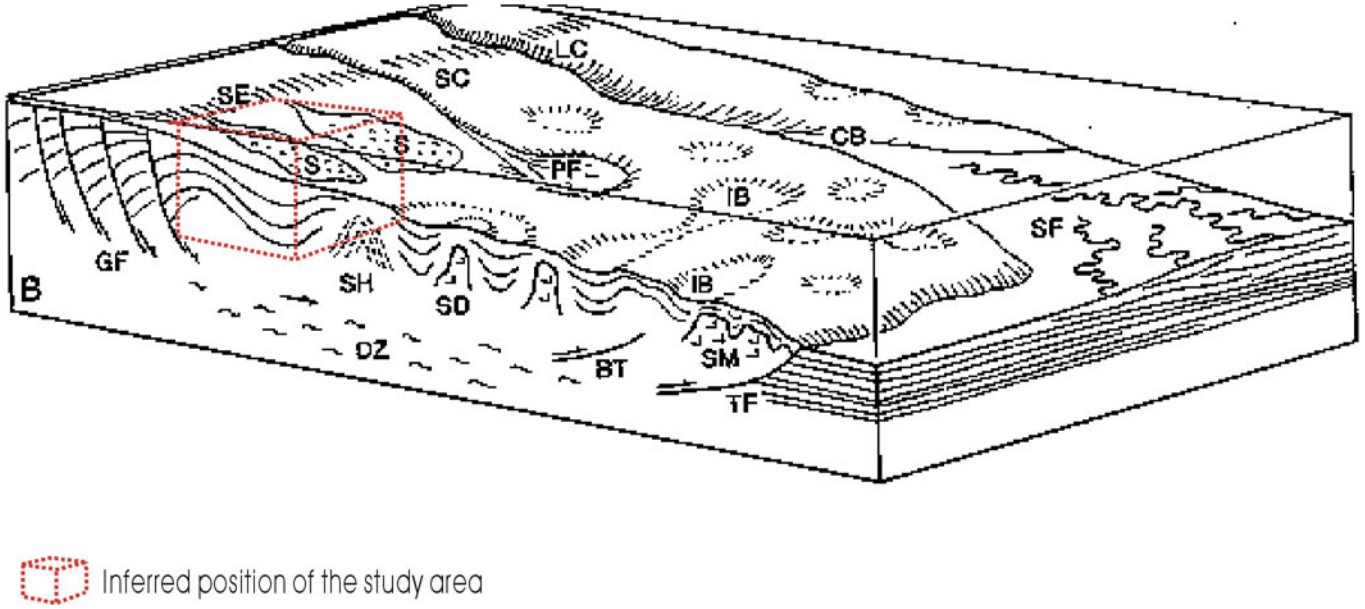

Figure 9. Unstable progradational shelf margin (modified from Winker, 1984). Labeled is the inferred basional position for the study area during Late Pliocene to Early Pleistocene.

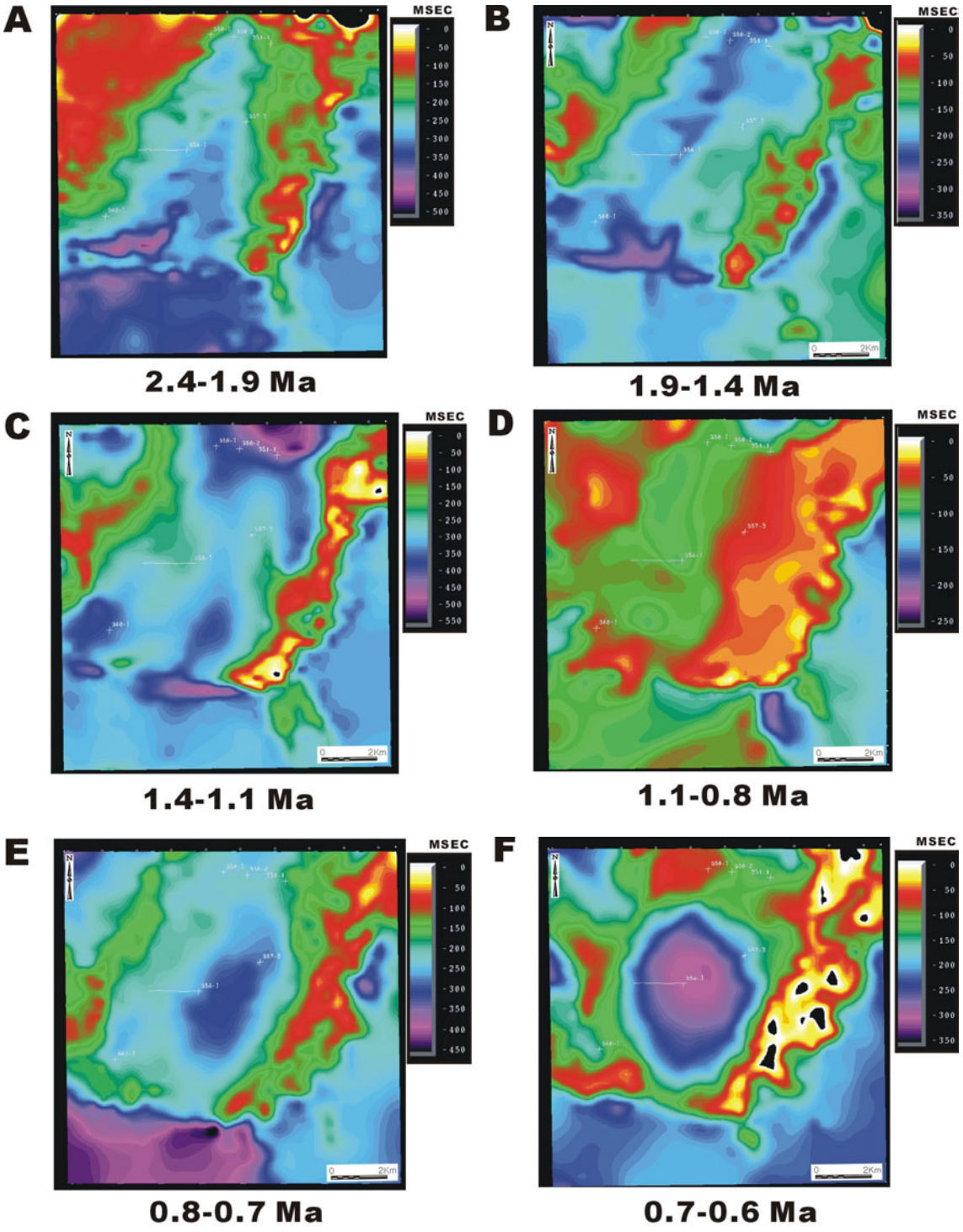

Figure 10. Isochron maps of the interpreted sequences.

3. SEQUENCE STRATIGRAPHY

3.1 Previous Works

3.1.1 Basic Concepts of Sequence Stratigraphy

Sequence stratigraphy is the study of genetic relationships of sediment bodies within a chronostratigraphic framework (Van Wagoner, et. al, 1990). The depositional sequence, which is the basic stratigraphic unit in sequence stratigraphy, is composed of genetically related sediment packages bounded by unconformities or their correlative conformities (Mitchum et al., 1977). Each depositional sequence is considered to have been deposited during one cycle of relative sea level change, and its boundaries usually form during the relative sea level fall (Mitchum and Van Wagoner, 1991). Depositional sequences consist of systems tracts. Brown and Fisher (1977) defined systems tracts as "the linkage of contemporaneous depositional systems." Each systems tracts is deposited during a specific phase of sea-level cycle and can be defined and characterized by its bounding surfaces, stratal geometry, position within the sequence, and stacking patterns of parasequences and parasequence sets (Haq, 1991). There are four types of system tracts: lowstand, transgressive, highstand, and shelf-margin systems tracts. Through sequence stratigraphic analysis, a chronostratigraphic framework can be built, upon which the prediction of lithologies and depositional environments of systems tracts are more or less possible (Vail, 1987). Therefore, sequence stratigraphic analysis should be performed prior to undertaking seismic facies analysis, and its applications with seismic facies analysis are especially useful to locate reservoir, source and seal rocks in any hydrocarbon explorations (Van Wagoner, et al., 1991).

3.1.2 Depositional Sequence in deep water setting

Figure 11 shows a schematic cross section with the stratal geometry and sequence stratigraphic relations in shelf-break and deepwater setting from the northern Gulf of Mexico (after Wagner et al., 1994). As the rate of eustatic sea level fall outpaces the rate of subsidence, the relative sea level starts to fall, accommodation space decreases, and shoreline retrogrades to basinward. When the relative sea level falls below or near shelf break, most of the shelf area is sub-aerially exposed and more terrigenous sediments are transported down to slope and basin floor as gravitational deposits. As the relative sea level rises again, the shoreline retreats to landward again, most sediments are confined in the shelf area and only pelagic and hemipelagic sediments can be deposited in the slope area. These pelagic and hemipelagic sediments are deposited very widely, draping the outer shelf, slope and basin floor with consistent thickness and resulting in a condensed interval.

The complete depositional sequence in deepwater environments has been described as a fining-upward succession of depositional strata, which is composed of basin floor fan, slope fan, prograding complex, and condensed section (Vail and Wornardt, 1990; Mitchum et al., 1990; Pacht et al., 1990; Yielding and Apps 1994; Villamil et al., 1998). Figure 12 shows the critical well-log pattern for the deepwater depositional sequence, in which the sequence boundary usually coincides with the first occurrence of the sand-prone sediment above the underlying shale-prone condensed section (Yielding and Apps, 1994). According to Mitchum et al. (1991), the prograding complex can be deposited from the shelf break to the distal part of the basin, in which it is thinning basinward. In the distal part of the basin, it might be difficult to differentiate the prograding complex from the underlying slope fan sediments due to the slow sedimentation rate in deepwater settings. Walker (1992) emphasized that the condensed sections usually directly overlie a basin floor fan and slope fan in the Mississippi fan area. Weimer et al. (1998) also reported that prograding complex, transgressive and highstand systems tracts are usually represented by condensed sections in slope basins

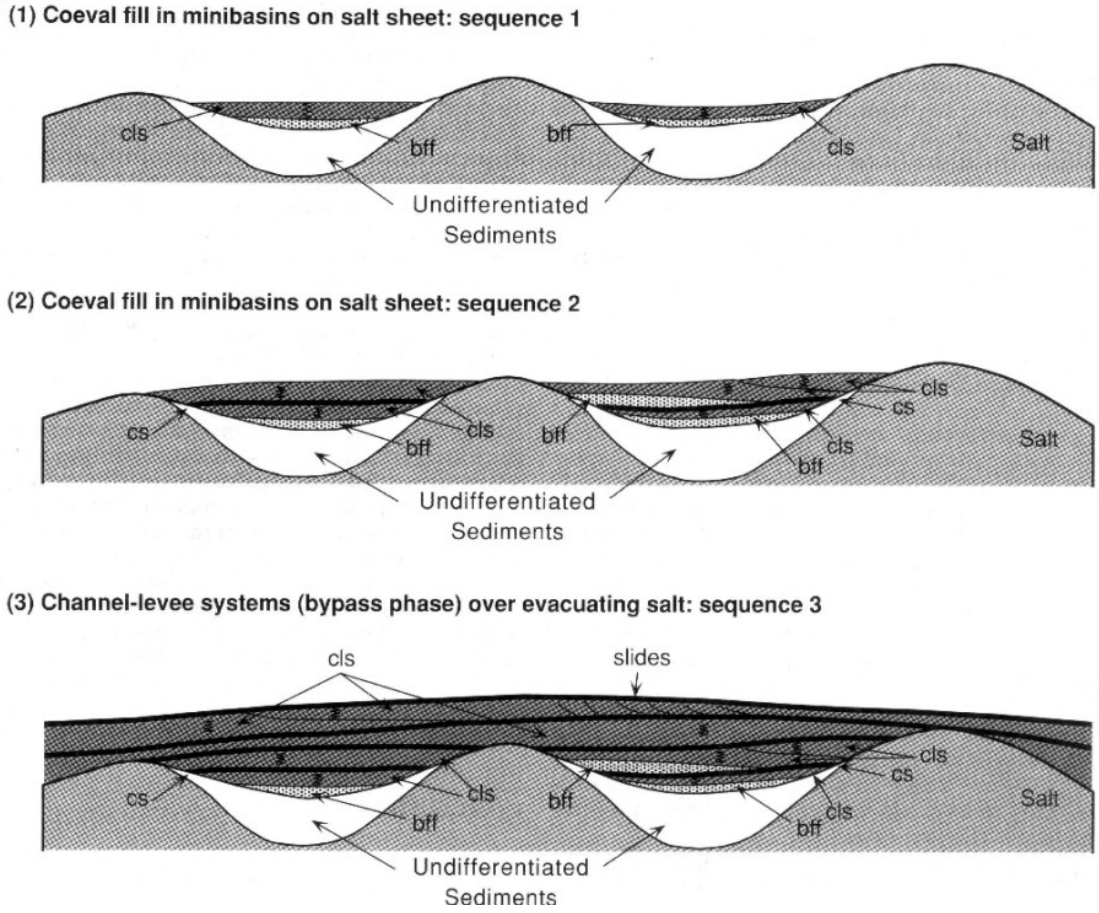

Figure 11. Depositional model in salt withdrawal mini-basin, Gulf of Mexico (after Weimer et al., 1998). cs: condensed section; cls: channel levee system; bff: basin floor fan.

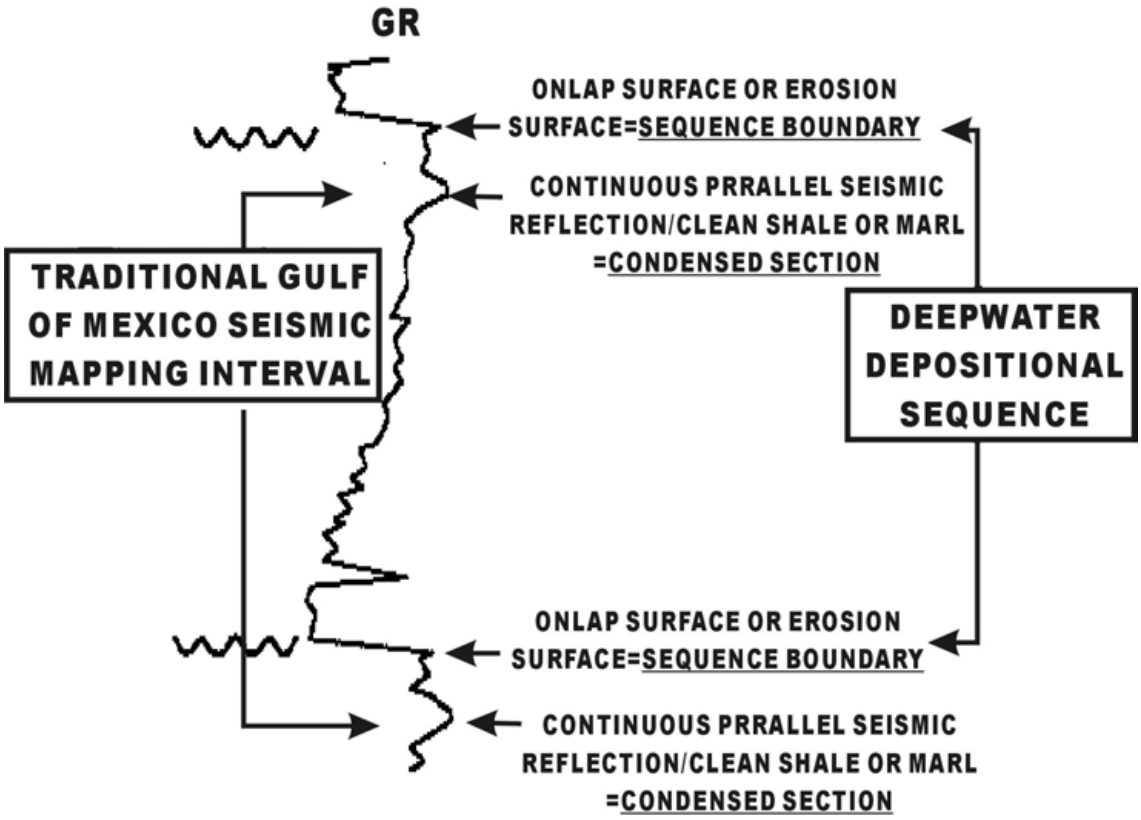

Figure 12. Schematic diagram showing the typical well-log expression of the deepwater depositional sequence in Gulf of Mexico (after Yielding and Apps, 1994).

in the Gulf of Mexico (Weimer et al., 1998). Therefore, basin floor fan, slope fan, and condensed sections commonly represent depositional sequences in deep-water environment.

3.2 Sequence Stratigraphic Analysis

3.2.1 Identification of Sequence Boundaries and Condensed Sections

As stated earlier, the depositional sequence in deep water setting usually consists of lowstand systems tracts and condensed sections deposited during the late stage of lowstand, transgressive and highstand systems tracts. Sequence boundaries in deepwater setting are not usually represented as erosional unconformities, but rather form parallel conformities to the underlying condensed intervals. They may be regarded as contact surfaces between the upper limit of condensed intervals and the base of the overlying lowstand systems tract. Therefore, it is valuable to identify condensed intervals prior to identifying sequence boundaries. For this study, well logs and biostratigraphic data were mainly used to identify condensed sections and sequence boundaries.

During the deposition of condensed sections, the starvations of terrigenous sediments occur in the deepwater environment. As a result, terrigenous sediments are very limited in deep water environment, and faunal abundance and diversity increase abruptly. Thus, fossil abundance and diversity curves are the most reliable sources in defining the condensed interval (Shaffer, 1990). Paleo-top information is the first downhole occurrence depth of a particular species in a borehole, which may not be its true extinction time (Vail and Wornardt, 1991). But empirical, paleo-top data occur in or near condensed sections, especially in the Gulf of Mexico (Shaffer, 1990). In this study, paleo-tops were widely used locating condensed intervals.

In well logs, condensed sections may be characterized by high radioactivity, high neutron porosity, low density, low sonic velocity, and low resistivity, because condensed sections mainly composed by hemipelagic or pelagic sediments that contain significant

amount of organic matter, and exotic elements such as sulphides, glauconite, phosphate, and iridium (Rider, 1995). The marine organic matter has usually very high uranium content, which is one of the radioactive elements measured by the gamma ray tool, so that condensed sections can be characterized by higher radioactivity than other mud dominant sediments (Figure 13). Figure 14 shows the cross-plot of gamma ray (GR), spontaneous potential (SP), and resistivity (ILD) logs of Well 358-1, where the magenta rectangle covering the area of high GR, high SP and low resistivity indicates possible condensed sections. However, the green rectangle covering the area of high GR, low resistivity and low SP value is interpreted as sand zones containing some radioactive materials. If only the GR log was used, this interval showing high GR but low SP values cannot be differentiated from the condensed intervals. In Well 358-1, the selected condensed intervals have high GR and SP, and low resistivity. In Well 351-1, the intervals having high neutron, high GR and low density are selected as condensed sections (Figure 15). Therefore, it is preferable to use whole suites of log data to identify condensed sections. Whole suites of logs were not available for all wells used in this study, so that only the well-log data available were used instead to define possible condensed intervals.

The locations of possible condensed sections identified using the cross-plot method were marked with biostratigraphic data including fossil abundance and diversity curves and paleo-tops for each well (Figures 16, 17 and 18). If these intervals selected from the well logs are well correlated with biostratigraphic data, they can be interpreted as condensed sections. In some intervals these two data are not well matched because of the difference between the resolutions of data sets used. The vertical resolution of the fossil data used for this study is no less than 90 ft as they were sampled every 90 ft, while the vertical resolution of the gamma ray tool is about 3 ft. Therefore, if the depth differences between well logs and paleo-top information are less than 90 ft, they can be accepted as the allowable margin of errors.

Sequence boundaries were interpreted based on the locations of condensed intervals and well log shapes. Condensed intervals located through the integrated

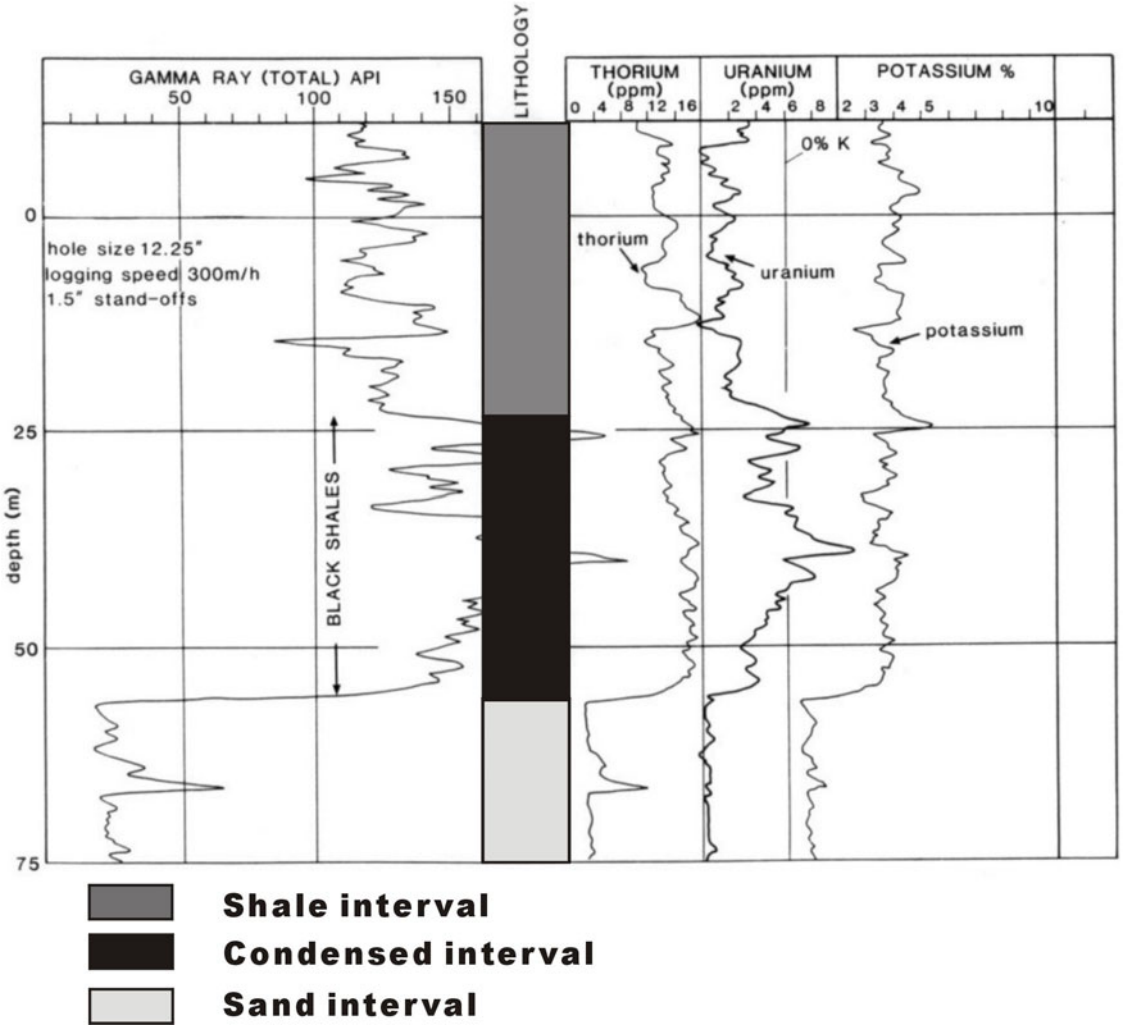

Figure 13. Characteristic log response for condensed interval (After Reider, 1995).

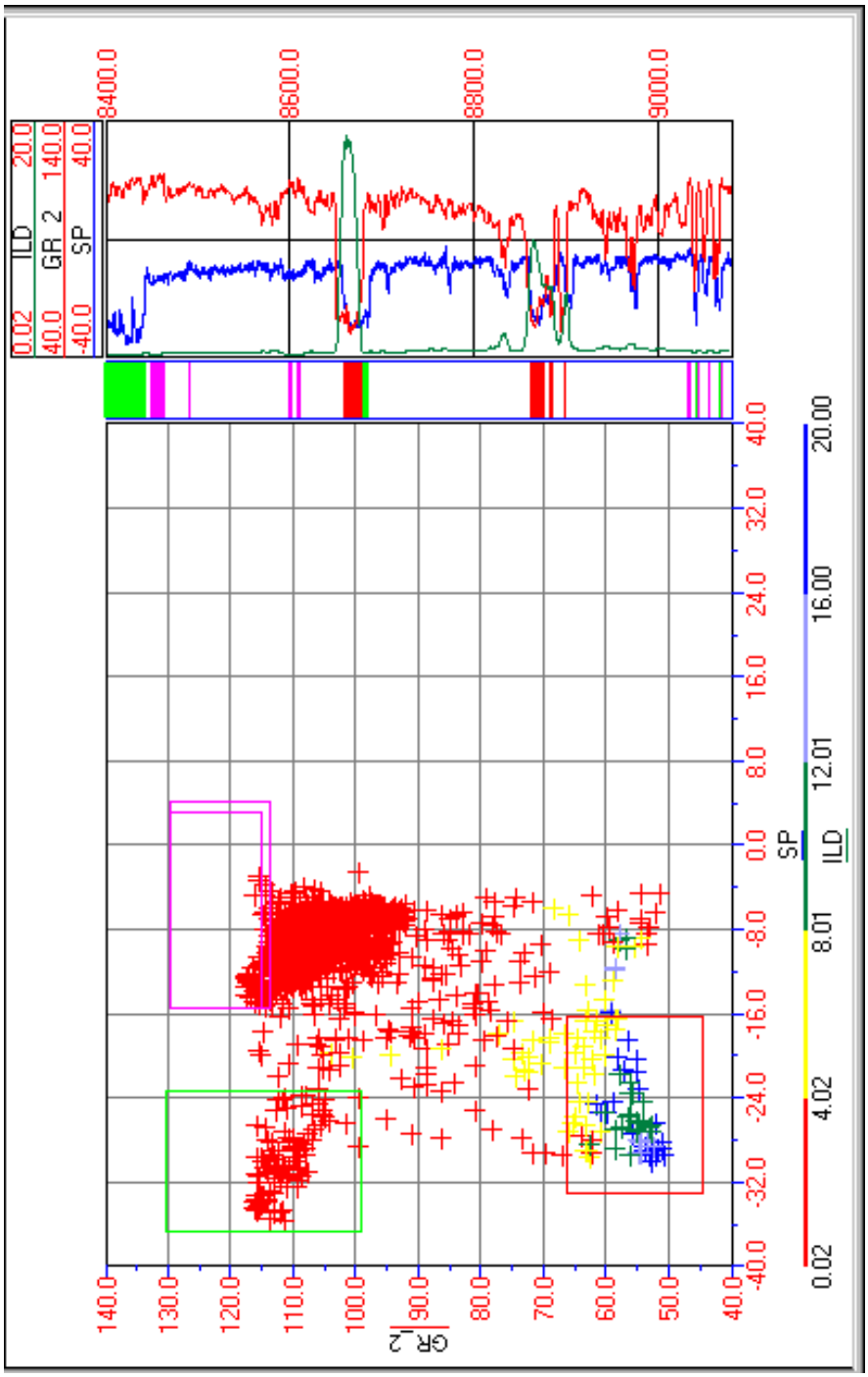

Figure 14. Cross-plot of GR, SP, and resistivity logs for Well 358-1. Purple square indicates the area of condensed section; green square indicate the area of low SP and high GR interpreted as radioactive sand; red square indicate the area of high resistivity, low SP, and low GR interpreted as possible hydrocarbon-bearing interval.

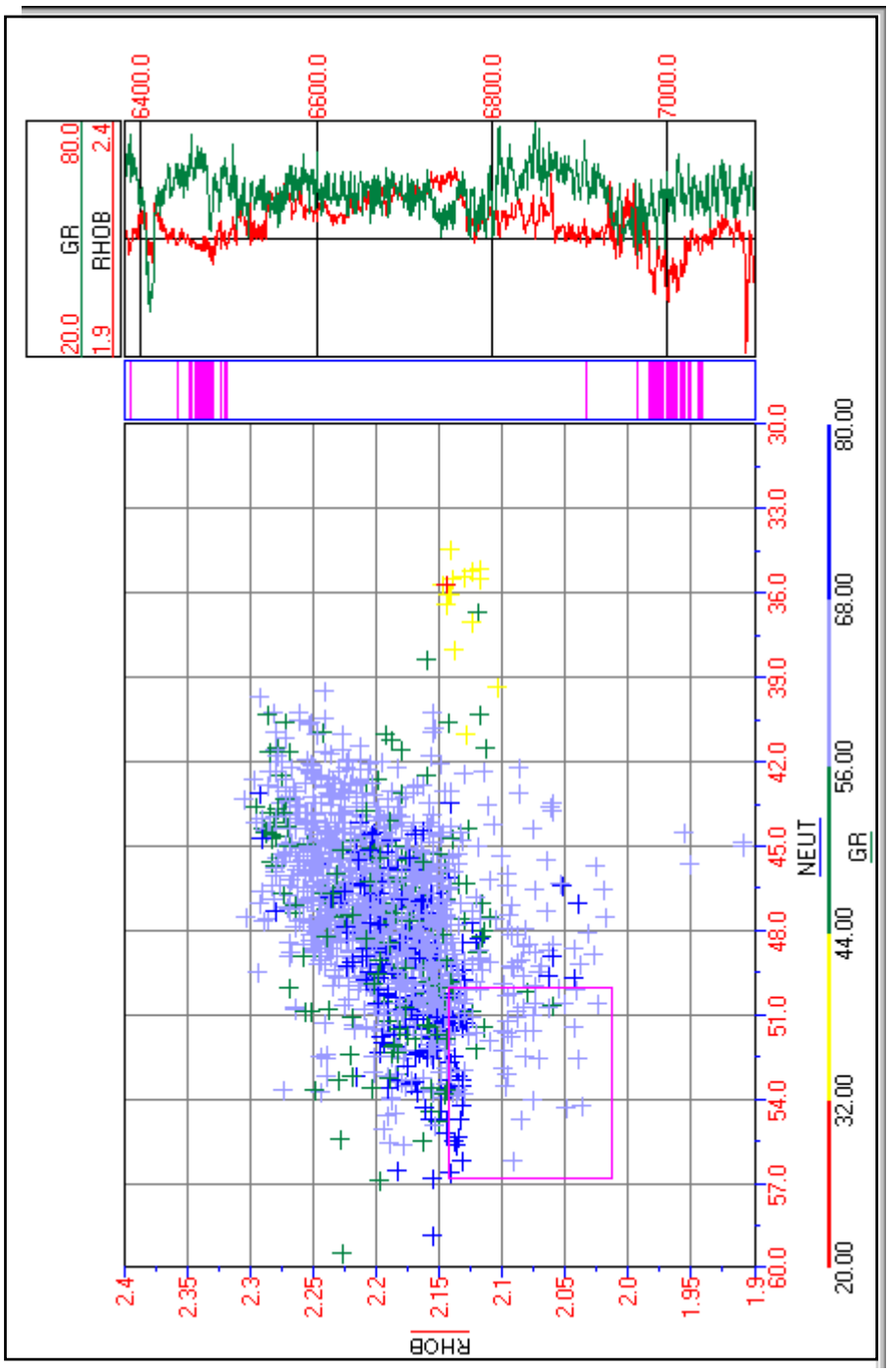

Figure 15. Cross plot of GR, density, and neutron logs for Well 351-1. The areas of purple are interpreted as possible condensed intervals with low density, high neutron and high GR.

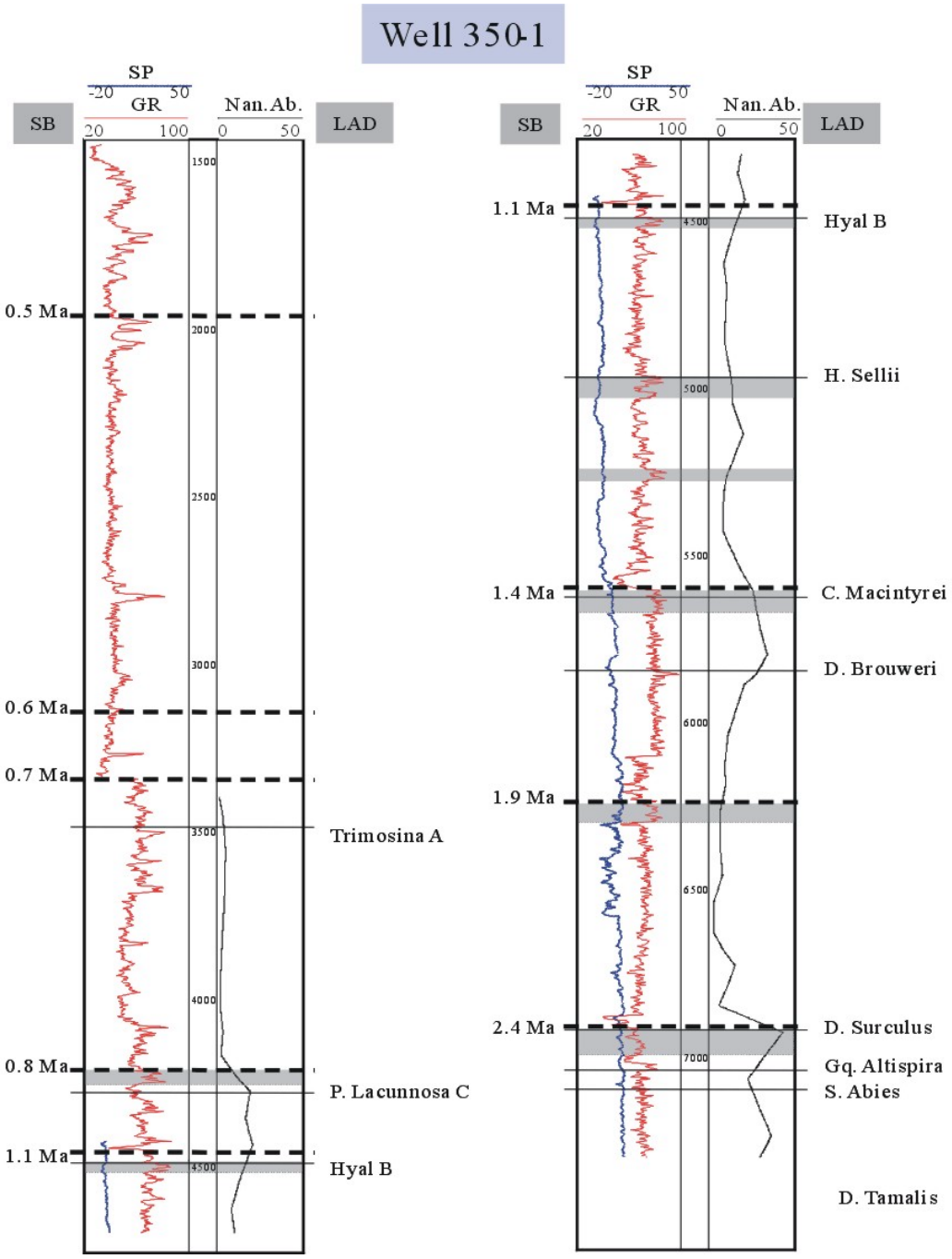

Figure 16. Condensed section (hatched interval) and sequence boundary (dashed line) interpretation for Well 350-1. SB: sequence boundary; LAD: last appearance datum; Nan Ab.: calcareous nannoplankton abundance.

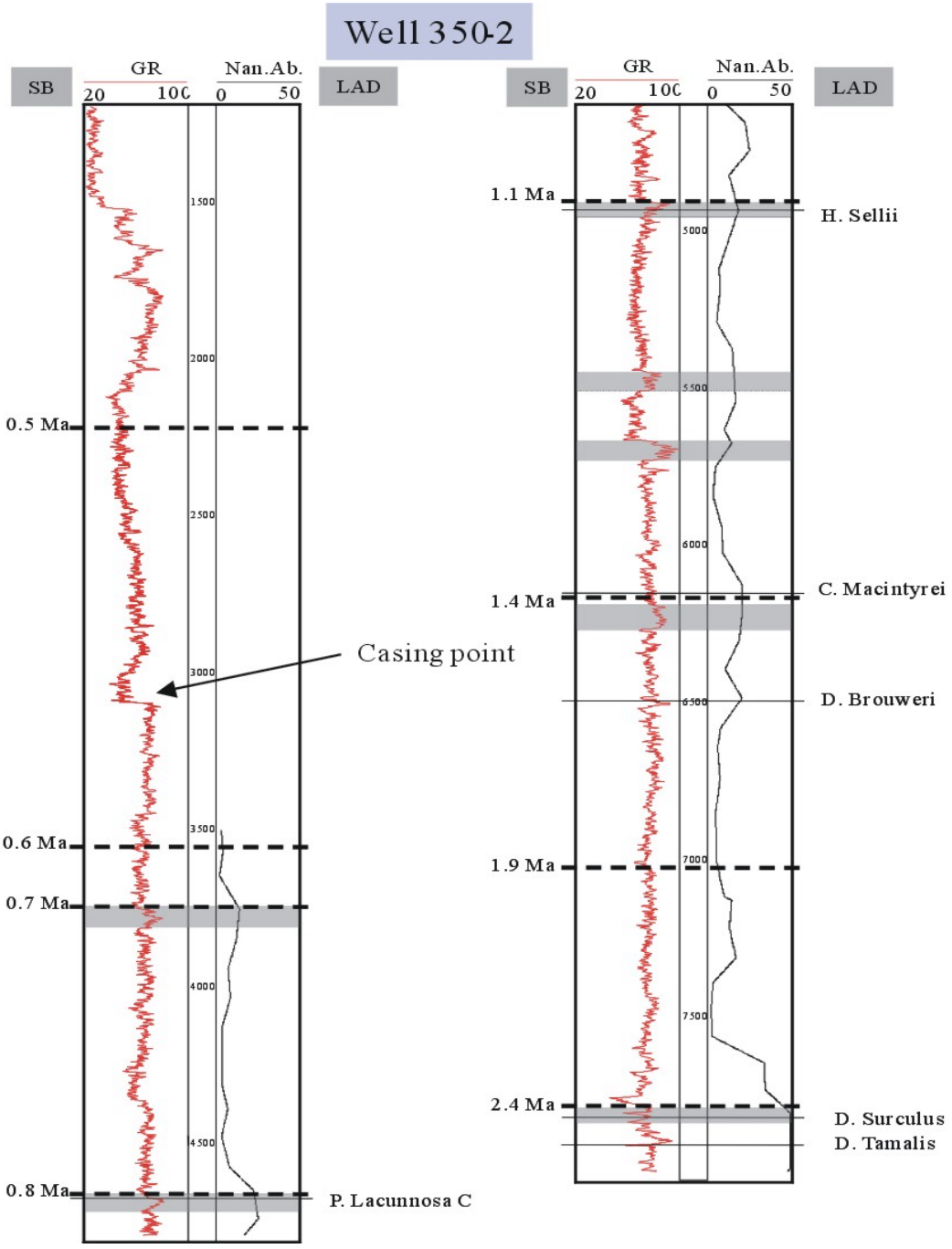

Figure 17. Condensed section (hatched interval) and sequence boundary (dashed line) interpretation for Well 350-2. SB: sequence boundary; LAD: last appearance datum; Nan Ab.: calcareous nannoplankton abundance.

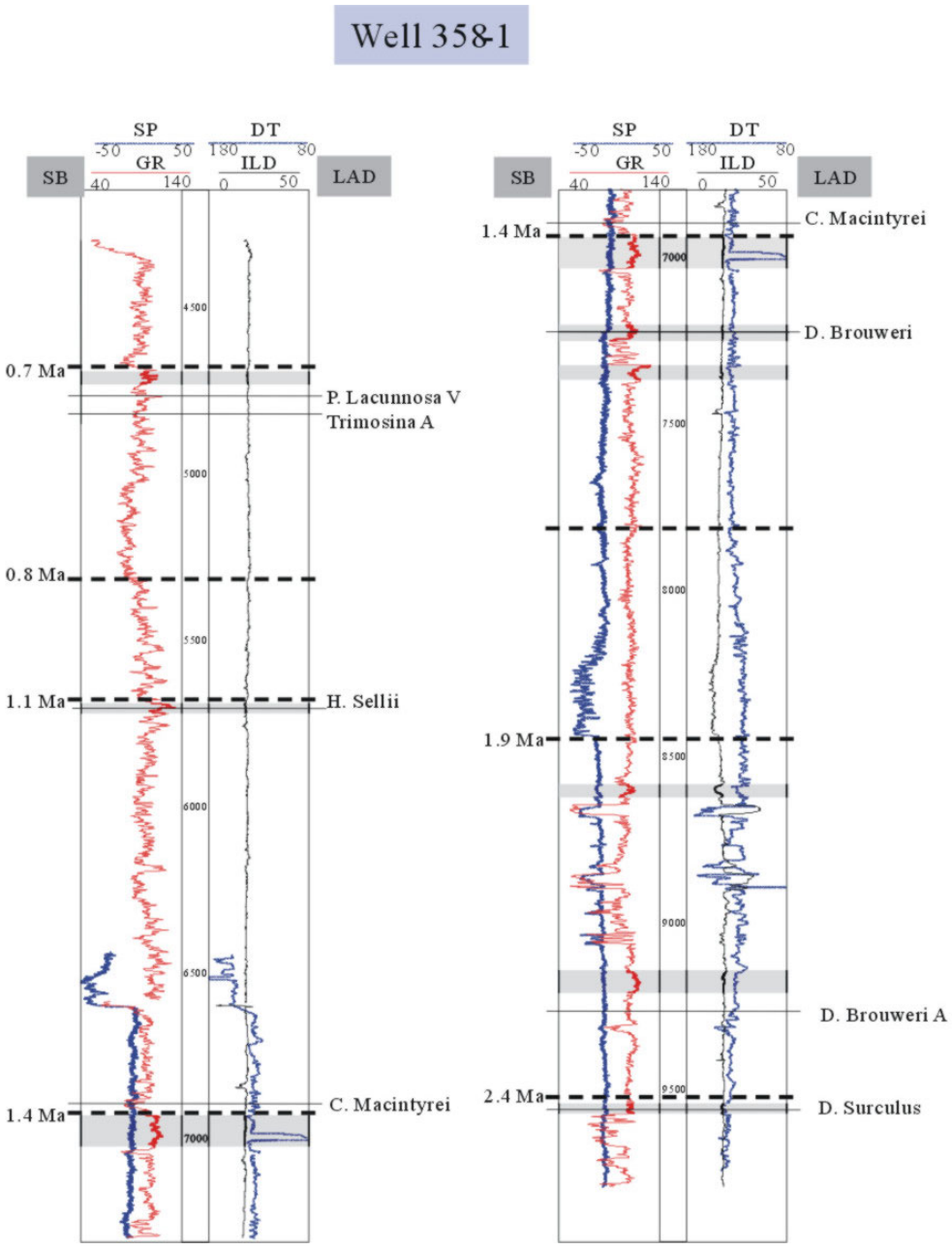

Figure 18. Condensed section (hatched interval) and sequence boundary (dashed line) interpretation for Well 358-1. SB: sequence boundary; LAD: last appearance datum; Nan Ab.: calcareous nannoplankton abundance.

approach using well logs and biostratigraphic data provided essential information to define sequence boundaries from the study area. The bases of sandy sediments occurring above condensed sections were interpreted as sequence boundaries (Figure 19). Some condensed sections occurring in the middle of shale-prone sediments are not related with sequence boundaries. In those cases, they are interpreted as internal condensed sections deposited on the slope fans. Internal condensed sections were observed in two sequences (1.9-1.4 Ma and 1.4-1.1 Ma sequences). Interpreted sequence boundaries from well logs and biostratigraphic data were correlated with 3-D seismic data using time-depth information (Figure 20). The interpreted sequence boundaries were usually matched with the reflectors with high amplitude and high coherency, which might be interpreted as condensed sections. On the seismic sections it is difficult to differentiate sequence boundaries from condensed sections because of the limited seismic resolution. The tops of the seismic reflectors corresponding to condensed sections were accepted as sequence boundaries and used to interpret 3-D seismic volume.

3.2.2 High-resolution Biostratigraphy and Cycle Charts

The recognized sequences can be correlated with the globally recognized cycle charts of the eustatic sea-level curves (Haq et al., 1988). The planktonic foraminifera and calcareous nannofossils are very important as the standard of reference for dating Late Cenozoic sediments on a global scale. However, the benthic foraminifera, whose habitat is largely controlled by facies and depositional environment, are much less reliable (Mitchum et al., 1990). Thus, they are used only when the other fauna information are not available. For this study calcareous nannofossils were preferentially used to define condensed sections and date the age of sequence boundaries. However, calcareous nannofossil data are available only for three wells (Table 1), so that for the wells for which nannofossils are not available, benthic foraminifera were used instead.

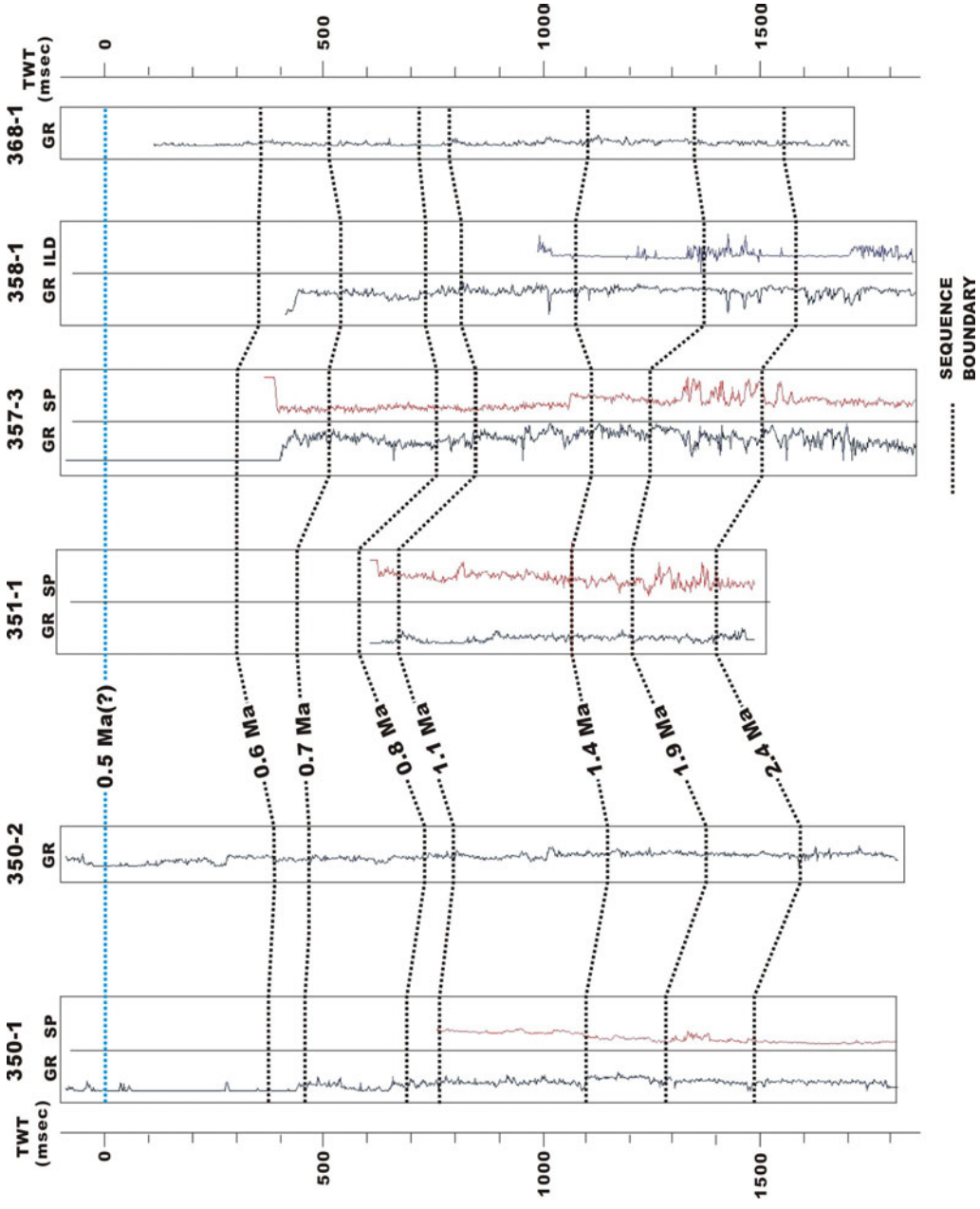

Figure 19. Well log correlation flattened by 0.5 Ma sequence boundary.

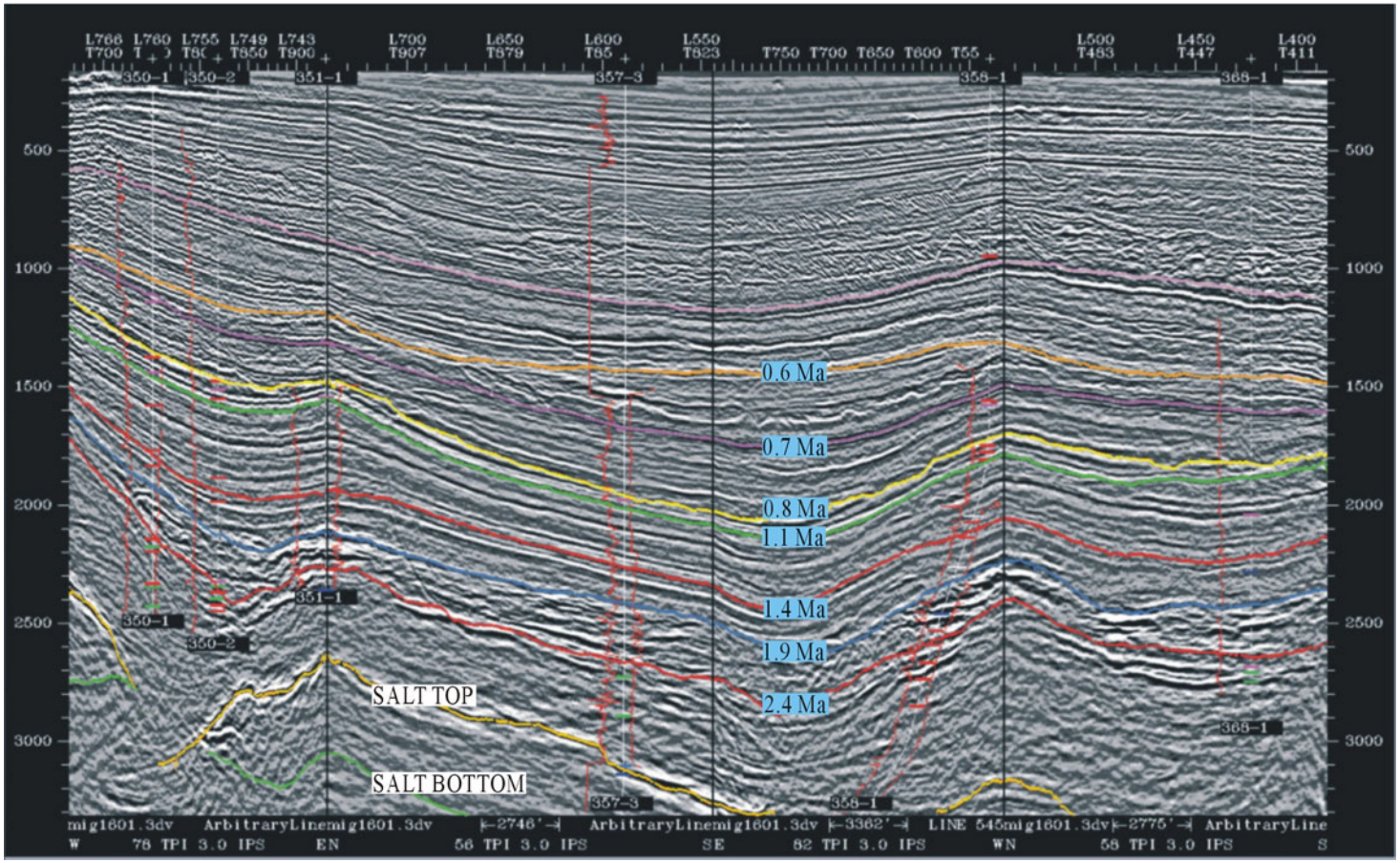

Figure 20. Seismic section crossing six wells showing sequence boundaries interpreted from well logs and biostratigraphic data. For each well paleo-tops and well logs including GR (left) and resistivity (right) are displayed. Paleo tops generally occur near the sequence boundaries. See Figure 1 for well locations.

Interpreted sequence boundaries were correlated with the Neogene biostratigraphic zonation and coastal onlap chart of the Gulf of Mexico (Figure 21: Paleo-Data, Inc., 1993). The periods of Plio-Pleistocene cycles from 5.5 Ma to 0.8 Ma are about 0.4 m.y. to 0.5 m.y.(third-order) and Late Pleistocene sediments younger than 0.8 Ma are characterized by very rapid glacio-eustatic cycles with periods of about 100,000 years (fourth-order). Four 3rd-order and two 4th-order sequences were interpreted from this study.

3.2.3 Sequence Stratigraphic Analysis

Regional sequence stratigraphic analysis including the study area has been performed and published by Weimer et al. (1998). However, no detailed stratigraphic study using 3-D seismic data was published. Seven sequence boundaries (2.4 Ma through 0.6 Ma) were interpreted mostly from paleo-tops, fossil abundance curves and well log data. Sediments older than the 2.4 Ma sequence boundary are not differentiable from seismic data, so they were excluded from this study. Also, the sequences above the 0.6 Ma, sequence boundaries could not be interpreted with confidence, because only limited well data and biostratigraphic data (only one well has paleo-top information for this age) were available (Table 1).

Most seismic sequences are convergent, thinning toward salt highs in the east-west direction and wedge-shape and thickening to basinward in the north-south direction (Figures 4 and 6). Overall, most sequences show a fining-upward pattern, in which coarse sediments tend to be deposited in the lower part of the sequence, and the upper parts of them are dominated by shale-prone sediment topped by hemipelagic and pelagic sediments (Figure 19). Sequences formed after 1.4 Ma sequence boundary consist of mud-prone sediments and condensed sections, for which the sedimentation of sand-prone deposits significantly decreased. Sea level change does not significantly affect deepwater environments where sediments are not subaerially exposed, even in low-sea

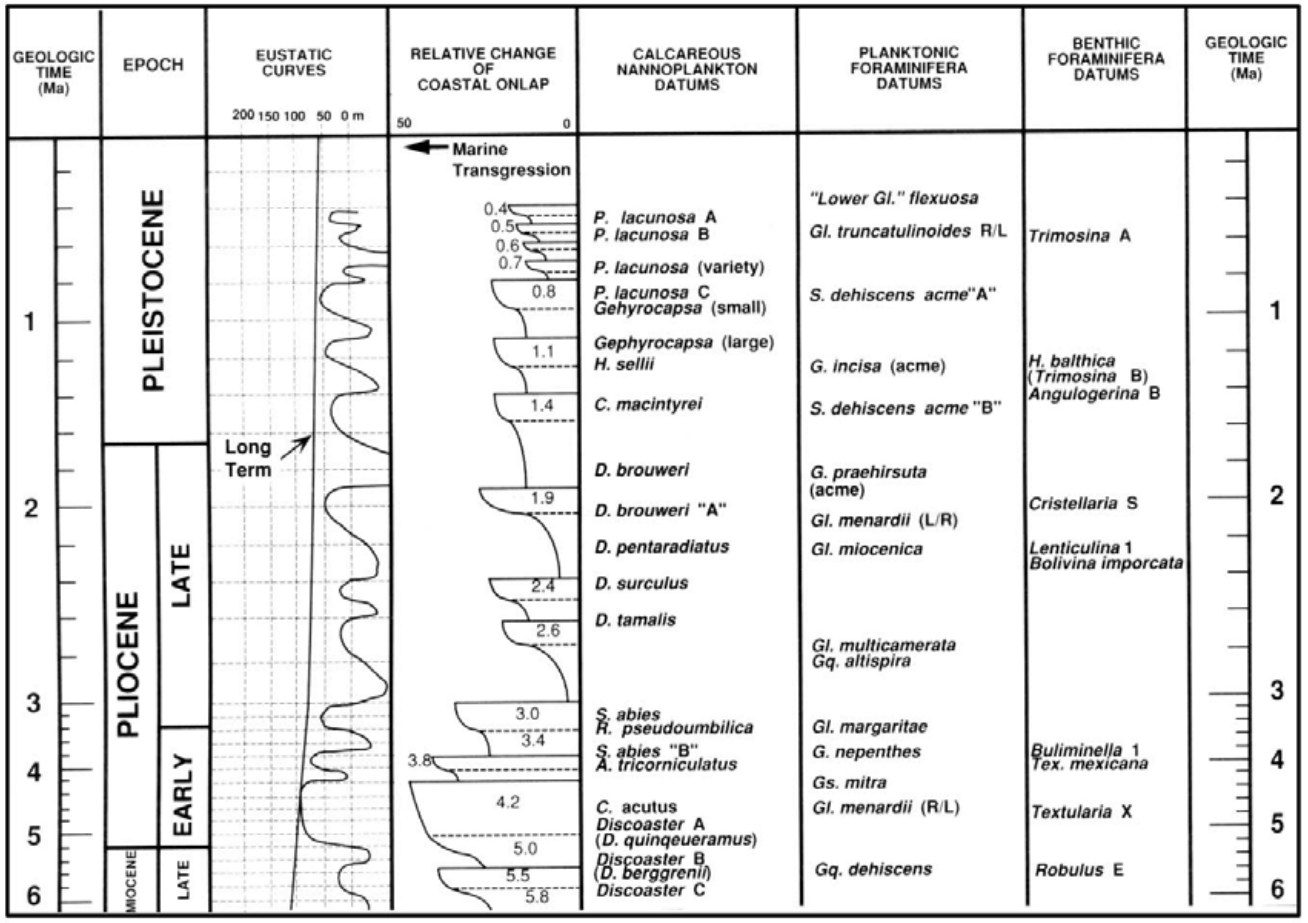

Figure 21. Plio-Pleistocene biostratigraphic zonation and coastal onlap curves, Northern Gulf of Mexico (after Paleo-Data Inc., 1993).

level stages. Overall, sequence boundaries are conformable with underlying and overlying sediments. However, some sequence boundaries were partly or fully eroded by overlying channel features (ex: 1.9 and 0.8 Ma sequence boundaries) or by bypass sediments or submarine canyons in the upper slope (ex: 0.6 Ma sequence boundary; Figure 20). The erosional surfaces caused by channel, slide, slump and debris flows are not stratigraphic unconformities in deepwater slope settings (Morton, 1993). Therefore, they should not be used as sequence boundaries without additional evidences.

After 0.6 Ma, salt evacuation from the central part of the basin resulted in infilling the salt-withdrawal basin, and the prograding shelf edge approached the study area. After 0.6 Ma, slump and slide sediments caused by shelf and slope failure were plentifully supplied and erosional surfaces caused by sediment bypass are commonly observed in upper slope area.

4. SEISMIC FACIES ANALYSIS

The definition of facies analysis is given by Anderton (1985) as the description and characterization of sediment bodies, which can be interpreted in terms of depositional process and depositional environment. For this purpose, sedimentary rocks can be classified by their specific characteristics such as lithology, composition, color, geometry, sedimentary structures, and fossil contents (Pirrie, 1998). Thus, seismic facies analysis can be defined as the study of the description and classification of seismic data into different seismic packages, which are distinguished by specified characteristics from adjacent reflectors. In seismic data, parameters like reflection configurations and various seismic parameters including amplitude, continuity, phase, frequency, and interval velocity are frequently used to describe and characterize these seismic units (Vail et al., 1997). These parameters can be used to infer the geological information on lithology and depositional process and environment, which is one of the main purposes of seismic facies analysis. Even though there is no unique relationship between specific seismic parameters and litho-facies, reasonable geological information such as depositional environment and lithology can be extracted from seismic facies analysis when combined with well logs, cuttings descriptions and paleo-data (Whittaker, 1998). In this study, seismic reflection characteristics including amplitude, coherency, and reflection configuration were examined for each sequence interpreted on vertical seismic sections, through which five distinctive seismic facies were identified (Figure 22 and 23).

In the conventional method, every seismic facies should be mapped in plan view to see its lateral variations and relationships each other. However, 3-D seismic volumes provide an easier and more effective method, called the horizon-slice technique, with which the lateral variations of the interpreted seismic facies in a certain time interval can be traced and described systematically. Seismic volume flattened by reference horizons including sequence boundaries or condensed sections is used for this purpose. These kinds of horizon slices are time equivalent surfaces and show the lateral

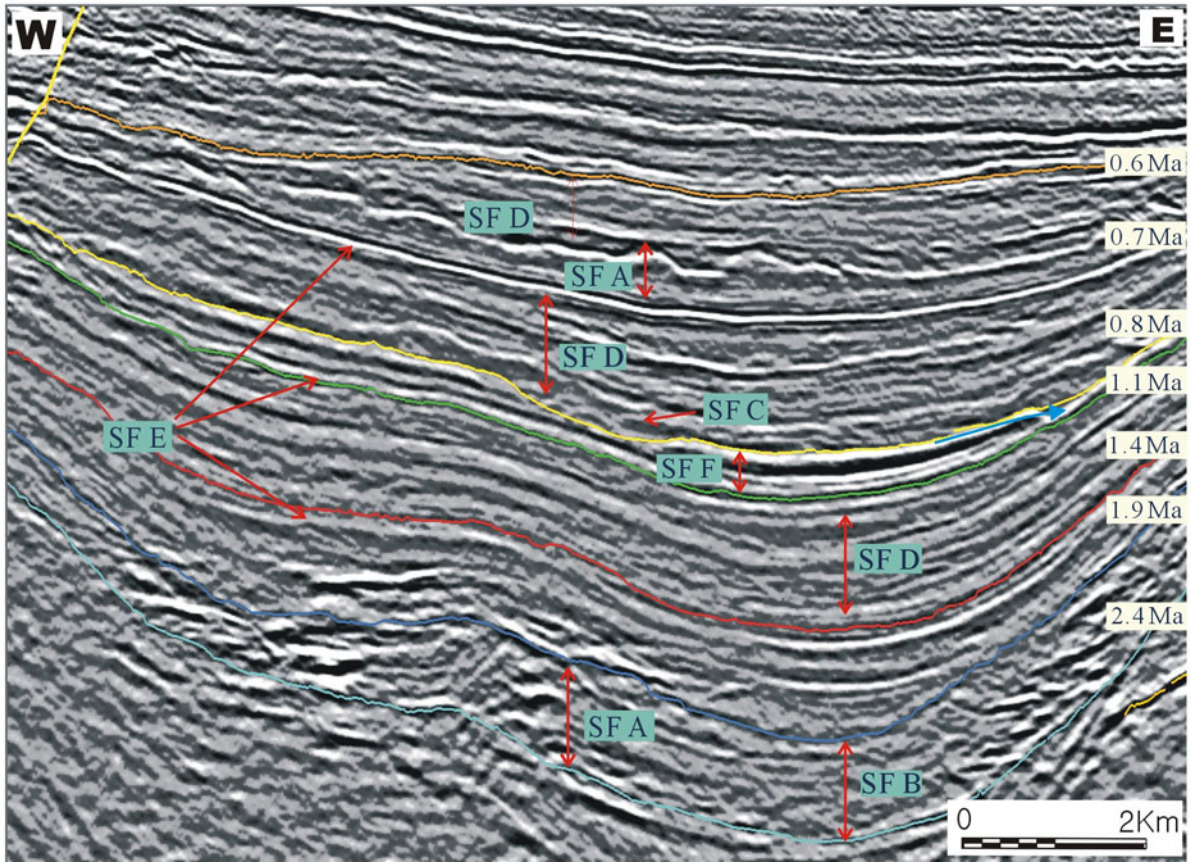

Figure 22. Seismic facies analysis from strike-oriented seismic section. See Figure 4 for location of seismic section. SF: seismic facies.

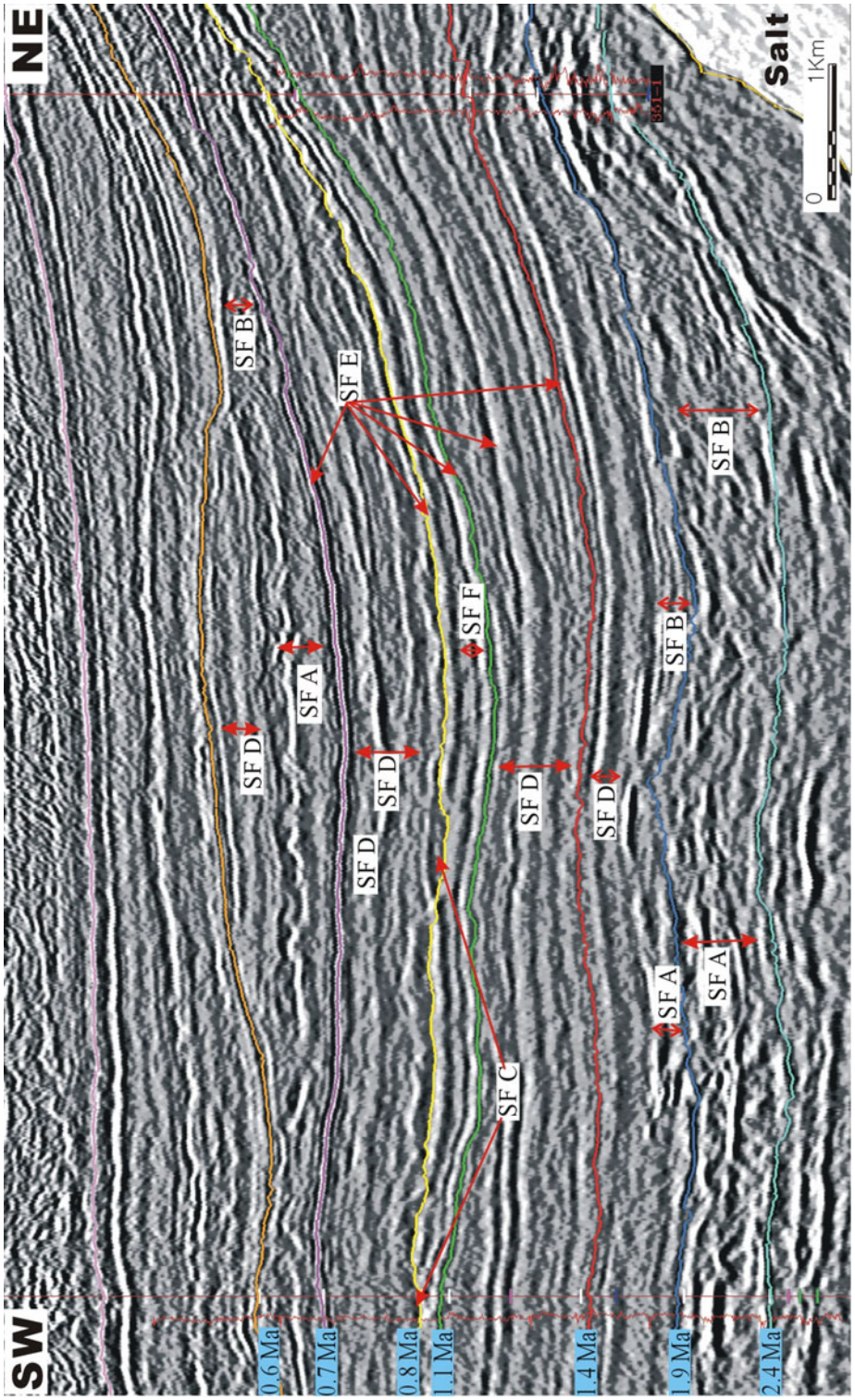

Figure 23. NE-SW trending seismic section showing the six seismic facies identified from the vertical seismic sections. See Figure 4 for location of seismic section. SF: seismic facies.

variations of seismic facies. When sequence boundaries were erosional surfaces, condensed sections were used as reference horizons to make slices parallel with the stratigraphic surfaces.

4.1 Vertical Seismic Facies

Seismic facies analysis was carried out for 6 sequences (2.4-1.9, 1.9-1.4, 1.4-1.1, 1.1-0.8, 0.8-0.7, and 0.7-0.6 Ma) using vertical seismic sections to cluster seismic data into different seismic facies that could be characterized by specific seismic parameters. The overall geometries of seismic facies were controlled by the paleo-geography. Six different seismic facies were defined based on amplitude, coherency, and reflection configuration and their seismic characteristics were described on the basis of vertical seismic sections (Figure 22 and 23).

4.2 Horizon Slices

Horizon slices were used to examine the lateral variation of the seismic facies. They are very effective to describe stratigraphic features, especially laterally confined sediments. Horizon slices were made using the interpreted sequence boundaries or condensed sections. The 3D seismic volume was flattened by reference horizons and then this flattened seismic volume was sliced parallel with reference horizons (Figure 24). As the thickness of each sequence changes significantly in the vertical section, horizon slices can be generated in the limited time interval from the reference horizons. The effective intervals are different for each sequence, but the interval decreases with the depth of sequences. If the horizon slices were cut obliquely to the seismic reflectors, the oblique cut might look like the real stratigraphic features. Therefore, the stratigraphic features interpreted from the horizon slices should be confirmed with the vertical seismic sections. Sequence boundaries showing erosional features cannot be used as reference horizons, because these surfaces are not parallel with the ancient stratigraphic surfaces,

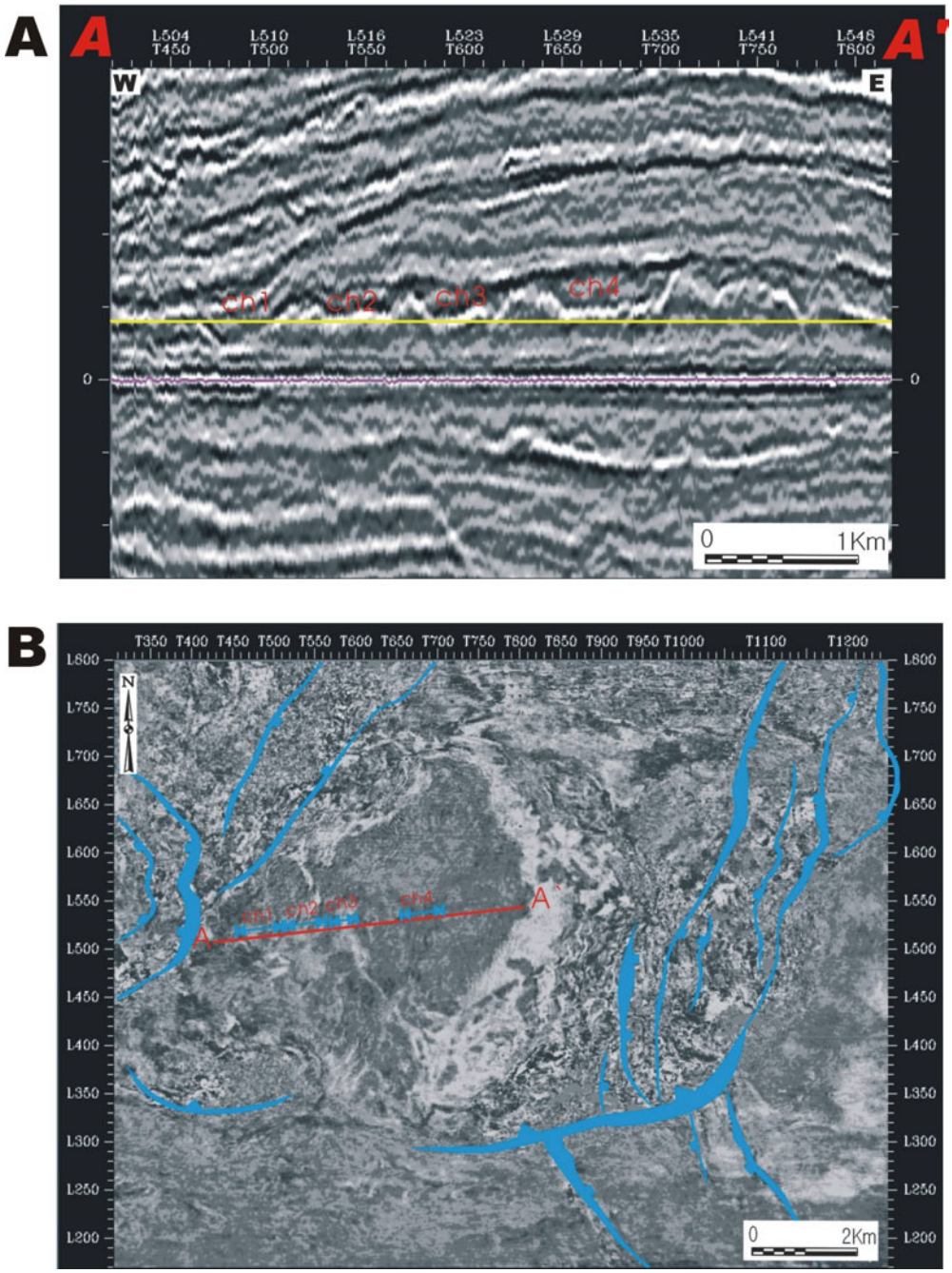

Figure 24. A: seismic section flattened by 0.7 Ma sequence boundary. Yellow line indicates sliced surface. B: horizon slice showing high amplitude area interpreted as depositional channel fills and surrounding low-amplitude area interpreted as overbank deposits in 0.7-0.6 Ma sequence. Shades of white indicate intensity of negative impedance and shades of black indicate intensity of positive impedance.

and horizon slices created by these surfaces cannot reveal the real stratigraphic features. Therefore, when sequence boundaries were erosional surfaces, condensed intervals were used as reference horizons instead to make horizon slice parallel with stratigraphic surfaces.

4.3 Seismic Facies Descriptions

Seismic Facies A

Seismic facies A is characterized by subparallel, high amplitude and poor coherence of reflectors containing concave upward pattern (Figures 22 and 23). This seismic facies commonly occurs in the lower part of the sequences (including 1.9 - 2.4 Ma, 1.4 - 1.9 Ma, 0.8 - 0.7 Ma, and 0.7 - 0.6 Ma) and especially well developed in the 2.4 -1.9 Ma sequence, which is interpreted as one of the most sand-dominant facies in the study area. The well logs for this facies usually show a bell or cylinder shape. On vertical seismic sections, this facies changes laterally to seismic facies B, which is characterized by subparallel, low-amplitude, moderate-coherence of seismic reflections. In plan view, they area represented by sinuously elongated high-amplitude areas trending NE-SW or NW-SE and usually surrounded by a low-amplitude area (Figures 24, 26, and 27).

Seismic Facies B

Facies B occurs in the 1.9 - 2.4 Ma, 1.4 - 1.9 Ma, 0.8 - 0.7 Ma, and 0.7 - 0.6 Ma sequences, located laterally near or adjacent to seismic facies A and characterized by subparallel, low-amplitude, moderate coherence of seismic reflection patterns (Figure 22 and 23). Well logs show mud-prone sediments deposited for these intervals, but serrated patterns were also observed when thin sands were intercalated (Figure 25). In horizon slices, this facies is represented as a broad, low-amplitude area without significant variation. Seismic facies A usually developed within this seismic facies (Figure 26 and 27).

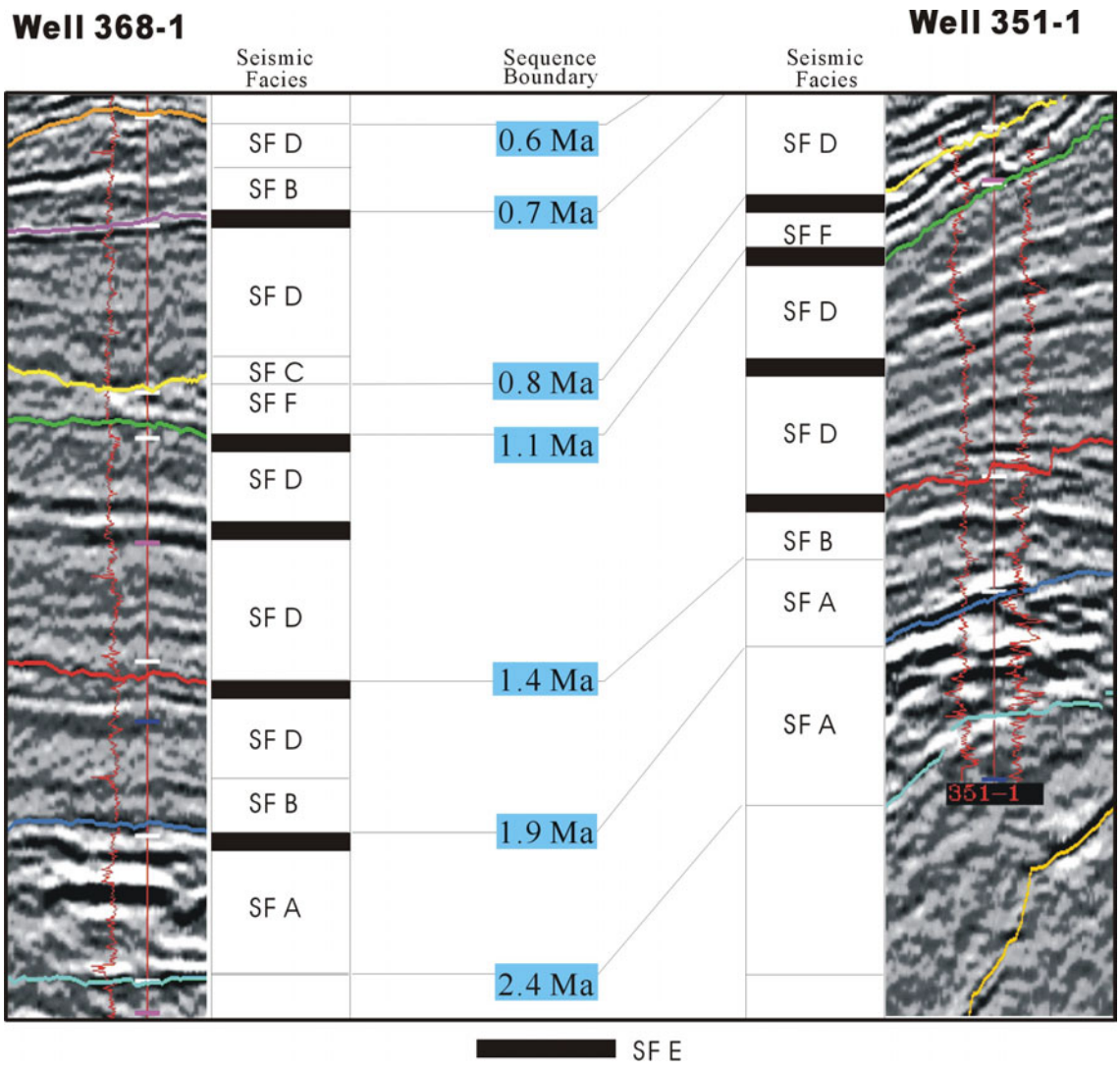

Figure 25. The correlation of seismic facies and their well-log responses. SF: seismic facies.

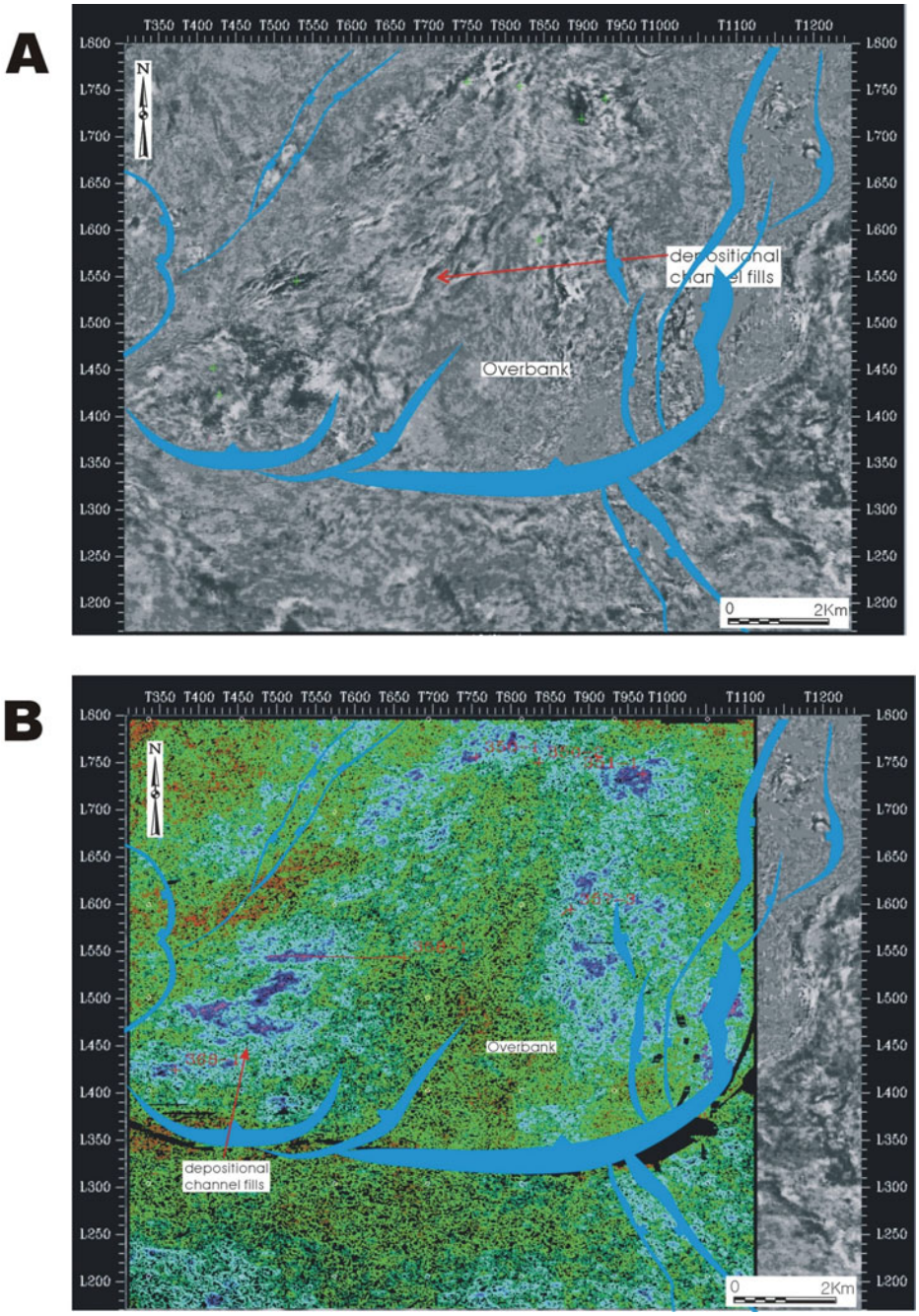

Figure 26. A: horizon slice showing depositional channel fills and overbank facies in 2.4-1.9 Ma sequence. B: RMS amplitude display. Purple indicates high-amplitude area interpreted as depositional channel fills and green indicates low-amplitude area interpreted as overbank area.

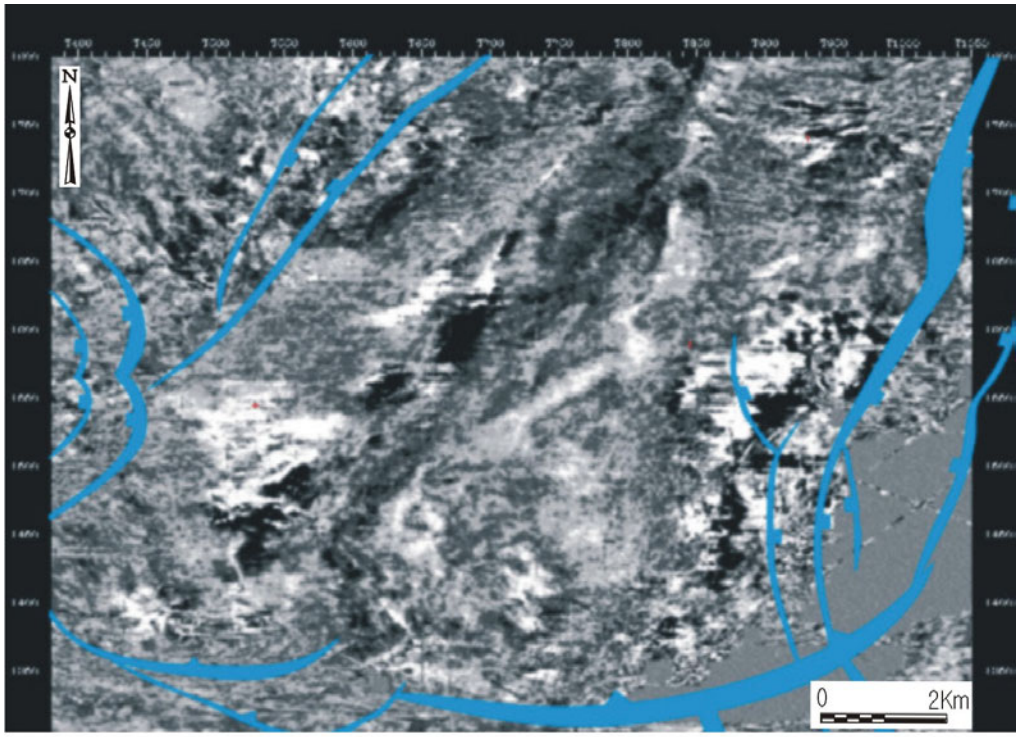

Figure 27. Horizon slice showing depositional channel fills and overbank facies developed in 1.4-1.1 Ma sequence. Shades of white indicate intensity of negative impedance and shades of black indicate intensity of positive impedance.

Seismic Facies C

Facies C is observed only in the 0.8 - 0.7 Ma sequence, where it is a concave-up erosional feature cut into the lower sequence boundary (Figures 22 and 23). The upper part of the underlying sequence was eroded and then was filled by a seismic unit characterized by a low amplitude, low coherency and subparallel pattern, interpreted as a mud-dominant facies. This seismic facies was formed in the early stage of lowstand in relative sea level and is much bigger in scale than seismic facies A. A horizon slices cut through this facies show that this facies trends from north to south and is filled by a low-amplitude area (Figure 28). It is less clear on horizon slice than seismic facies A and defined as low amplitude area with linear features surrounded by a high-amplitude area. Well 368-1 only penetrated this facies where well log responses indicate a mud-dominant sedimentation (Figure 25).

Seismic Facies D

Seismic facies D is characterized by parallel-to-subparallel, low amplitude, high coherency patterns that are commonly deposited above seismic facies A and B and underlain by seismic facies E (1.9 - 1.4 Ma and 1.4 - 1.1 Ma sequence). This facies is deposited widely over the basin and filled the basin with mud-dominant sediments. The typical shape of well logs from this facies is similar with the well log patterns from seismic facies B, which is represented as a thick shale interval; but when thin channel sands are intercalated, serrated pattern will occur. In plan view, facies B is characterized by a broad, low-amplitude area without significant amplitude variations (Figure 29).

Seismic Facies E

Facies E is described by parallel, high-amplitude, high-coherency of seismic characteristics (Figures 23 and 24). It shows very continuous thickness throughout the study area, indicating that its external shapes were not controlled by paleo-geometries. These seismic patterns are mainly observed in the uppermost part of each sequence and underlain directly by sequence boundaries. In horizon slices, this facies is represented

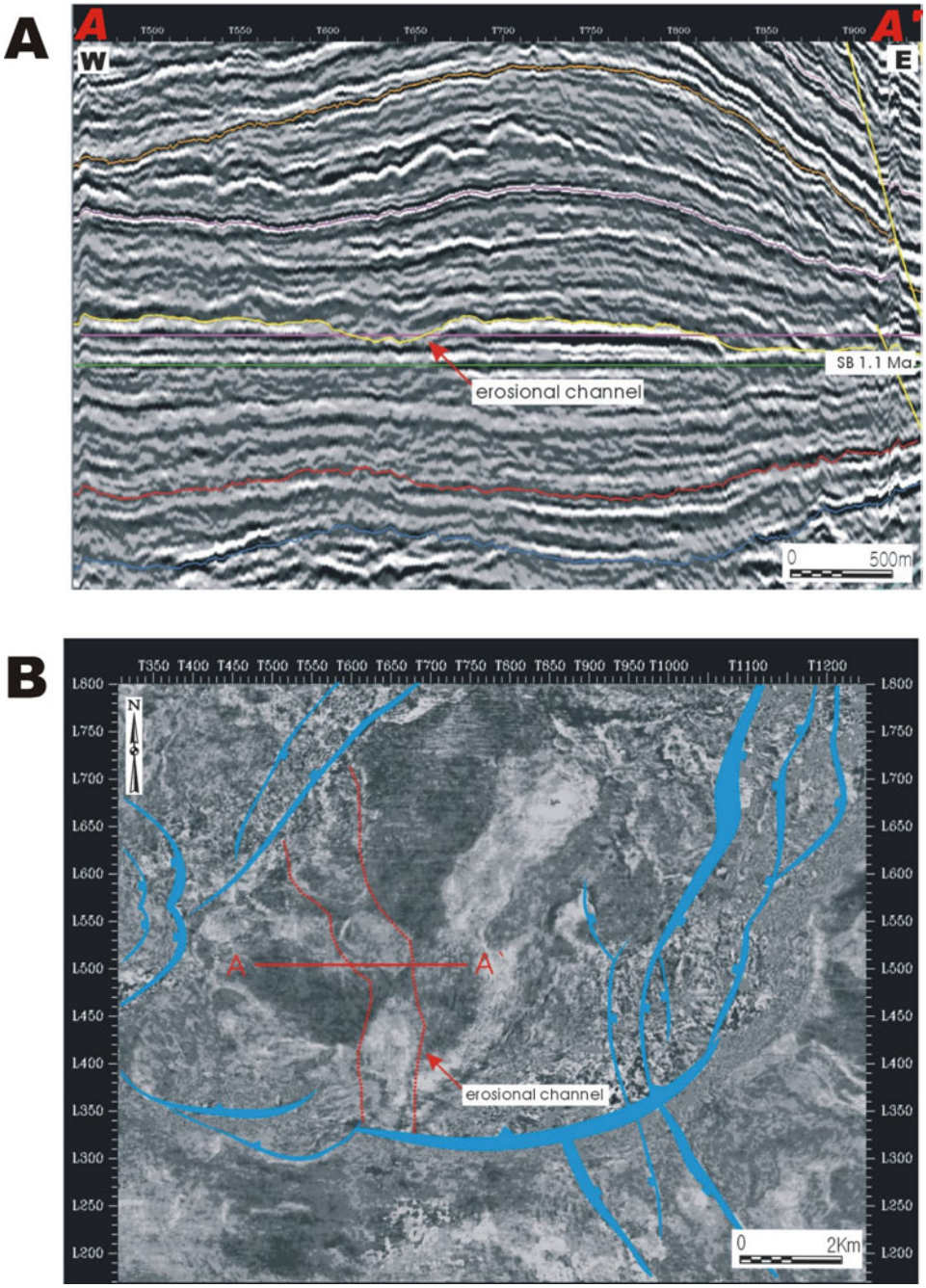

Figure 28. A: seismic section flattened by 1.1 Ma sequence boundary showing erosional channel. B: horizon slice showing N-S trending linear feature with low amplitude, interpreted as an erosional channel fill. Shades of white indicate intensity of negative impedance and shades of black indicate intensity of positive impedance.

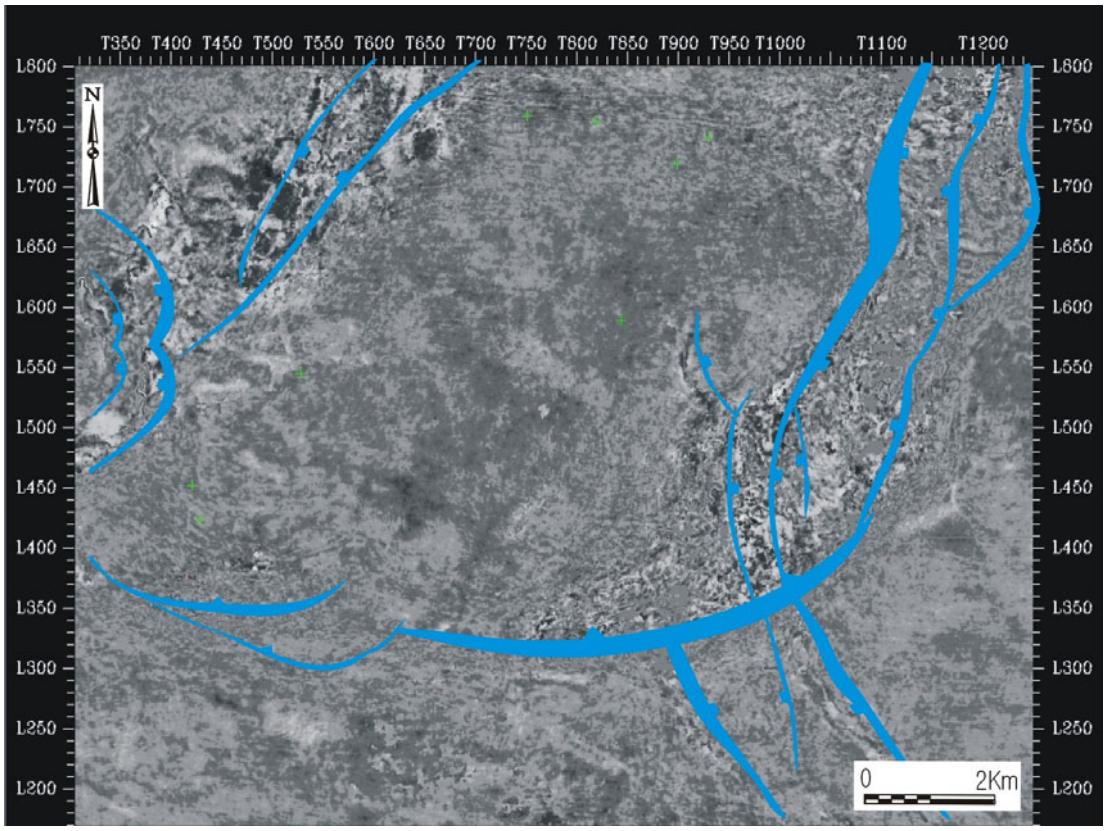

Figure 29. Horizon slice showing mud turbidite fills and sheets developed in 1.9-1.4 Ma sequence. Shades of white indicate intensity of negative impedance and shades of black indicate intensity of positive impedance.

as widespread, high-amplitude area (Figure 30). In well data, it is represented as high gamma ray and high fossil contents and diversities interpreted as condensed section (Figures 25 and 16-18).

Seismic Facies F

Seismic facies F is observed only in the lower part of 1.1-0.8 Ma sequence, where it is overlain by seismic facies E. It shows the seismic reflection characteristics of high amplitude and high coherency with mound-shape features. This mound-shaped feature downlaps onto the underlying sequence boundary (Figure 31). In the horizon slices, it is represented by a limited high-amplitude area. In the southern and eastern parts of the basin, its boundary was interpreted, but to the north and west it was not clear. In Figure 31, its amplitude value changes from peak to trough because its thickness becomes thinner to the westward. Its termination boundary is interpreted using both vertical seismic sections and horizon slices. This facies is expected to be composed of sand prone sediment represented by blocky well logs, but all wells available penetrated the marginal parts of this facies and their log responses show no distinct sand packages.

4.4 Facies Models and Depositional Environments

The intraslope basin in the Gulf of Mexico was mainly filled by sand and mud turbidites and pelagic and hemipelagic sediments (Bouma et al., 1990). Mutti and Normark (1991) described turbidite systems deposited in slope basins by five different turbidite elements that are basic building blocks of turbidite systems and can be recognized and mapped in marine, outcrop, and subsurface studies (Mutti and Normark, 1991). Turbidite elements can be explained as the genetic facies or facies associations that can be distinguished from adjacent strata and are commonly found from ancient and modern turbidite systems (Mutti and Normark, 1991). Their turbidite elements include (1) major erosional features, (2) channels, (3) overbank deposits, (4) lobes, and (5) channel-lobe-transition deposits. In 1998, Galloway defined slope basin turbidite

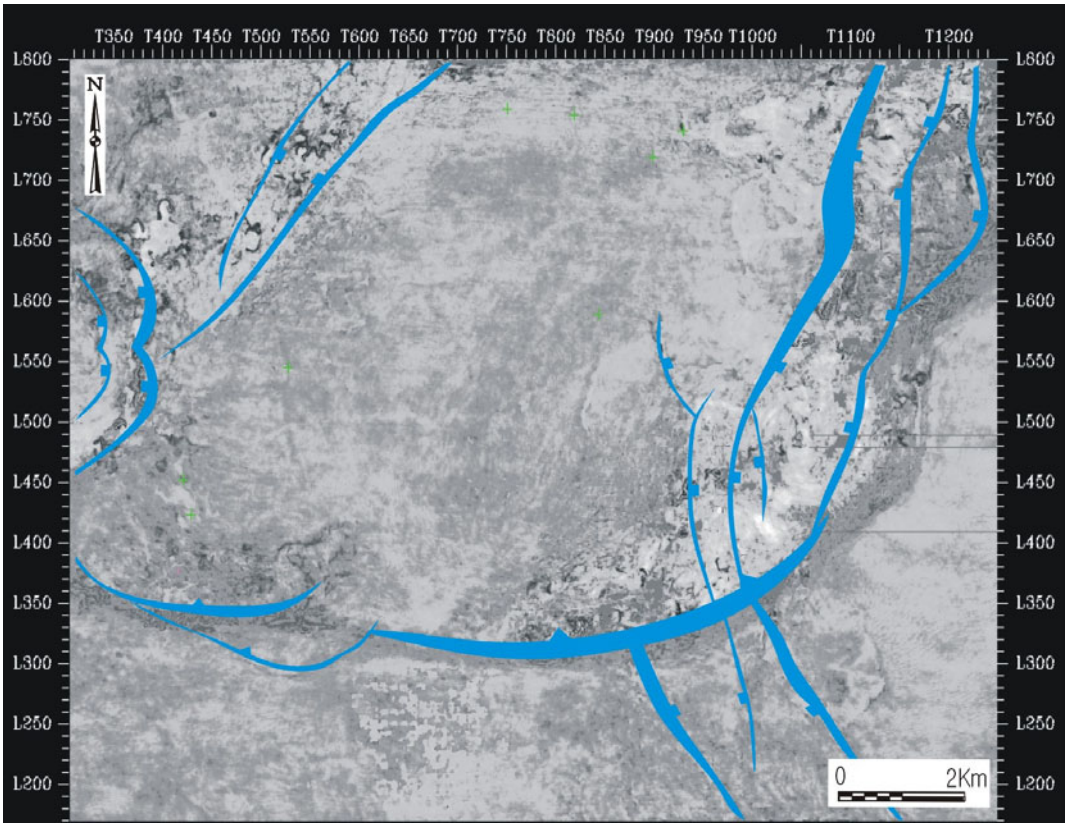

Figure 30. Horizon slice showing hemipelagic and pelagic fills from 0.8-0.7 Ma sequence. Shades of white indicate intensity of negative impedance and shades of black indicate intensity of positive impedance.

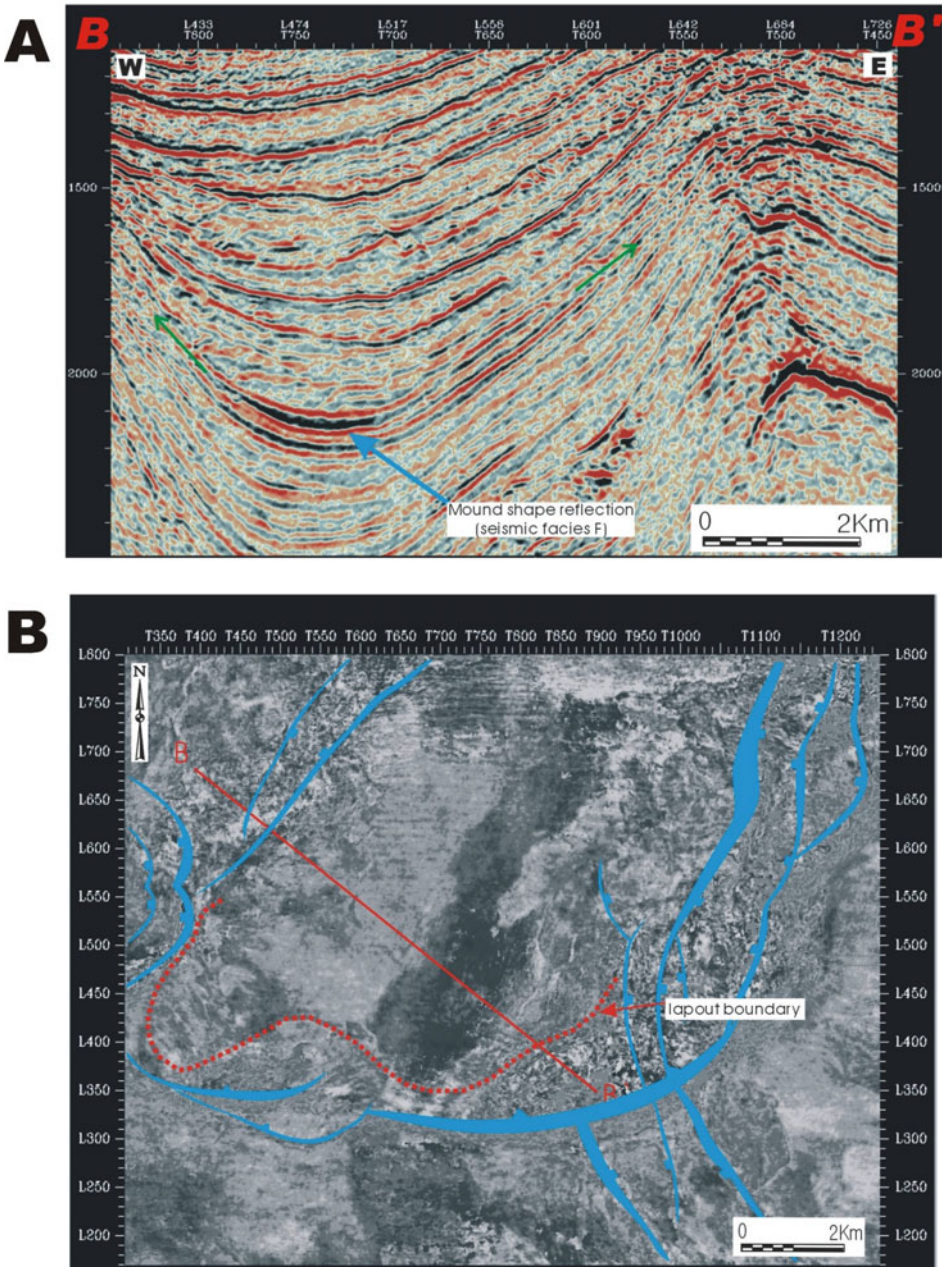

Figure 31. A: seismic section showing turbidite lobe sediment downlapping onto underlying sequence boundary. B: horizon slice showing turbidite lobe developed in 1.1-0.8 Ma sequence. Red dotted line indicates the edge of the turbidite lobe interpreted from vertical seismic section and horizon slice. Shades of white indicate intensity of negative impedance and shades of black indicate intensity of positive impedance.

systems into seven basic turbidite facies: (1) turbidite channel fills, (2) turbidite lobes, (3) sheet turbidite, (4) slide, slump, and debris-flow sheets, lobes and tongues, (5) fine-grained turbidite fills and sheets, (6) contourite drifts, and (7) hemipelagic drapes and fills. Though Galloway did not use the term "turbidite element" in his paper, the meaning of his turbidite facies can be regarded as same one as Mutti and Normark's.

This study used the term "turbidite element", but Galloway's classification was generally accepted with some modifications that were added to describe the turbidite system more efficiently. Seismic facies interpreted with the seismic sections and horizon slices were integrated with lithologic information to correlate with turbidite elements (Table 2). During 2.4 - 0.6 Ma, six different seismic facies were identified from seismic facies analysis and these seismic facies were interpreted into five types of turbidite elements: (1) depositional channel fills and overbank deposits, (2) erosional channel fills, (3) mud-turbidite fills and sheets, (4) turbidite lobes, and (5) pelagic and hemipelagic drapes (Table 2).

4.4.1 Depositional Channel and Overbank Deposits

Depositional channel and overbank deposits are the most common sand-prone turbidite elements in the study area. Depositional channels are dominantly developed in the lower slope and base of slope, where gravity flows decelerate (Galloway, 1998). Three depositional channels and overbank deposits were identified from the study (Figure 32). During the 0.7-0.6 Ma sequence, the study area is inferred to have been located in the mud-dominant upper slope environment, in which a typical levee channel overbank system could be deposited. These levee channels are highly sinuous, characteristics of a very low gradient and mud-dominant depositional slope (Clark et al., 1992).

Their lateral variations are very well defined by a series of horizon slices (Figure 33), which proves that the horizon-slice method is invaluable to define the geometries of channels. Two depositional channels trending NNE-SSW and NW-SE directions were described by Figure 33. The other depositional channels are deposited in 2,4-1.9 and 1.9-

Table 2. Seismic facies and characteristics of turbidite elements.

Seismic facies	*Seismic facies from vertical seismic sections*	*Seismic facies from horizon slices*	*Well log patterns and lithology*	*Turbidite Element*
A	High amplitude, low coherency and concave upward	Elongated sinuous, high amplitude area surrounded by broad low amplitude area	Bell or blocky shape	Depositional channel fills
B	Low amplitude, moderate coherency, and sub parallel	Broad low amplitude area occurring with sinuous high amplitude area	Mud dominant or serrate pattern	Overbank
C	Low amplitude, low coherency and sub parallel with concave upward shpae	Linear low amplitude area surrounded by high amplitude area	Mud dominant or serrate pattern	Erosional channel fills
D	Parallel, low amplitude, and moderate coherency	Broad fair to low amplitude area without significant variations	Mud dominant or serrate pattern	Mud turbidite fills and sheets
E	Parallel, high amplitude, high coherency	Wide spread high amplitude area	"Hot shale" (hemipelagic and pelagic shale)	Hemipelagic and pelagic drapes
F	Mound shape, high amplitude, high coherency	Limited high amplitude area	Cylinder types expected but no wells penetrated in this area (sand prone)	Turbidite lobes

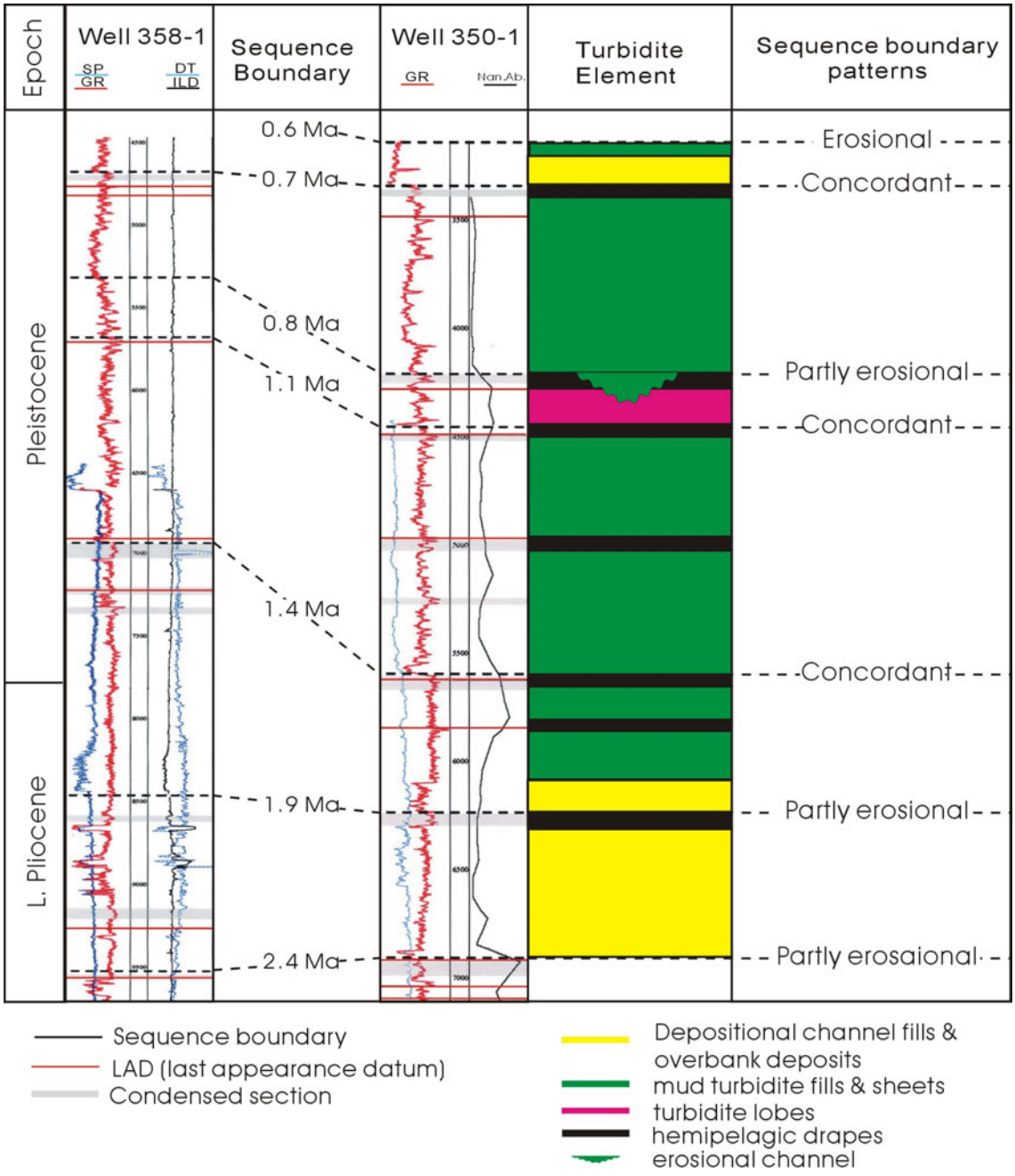

Figure 32. Vertical stacking patterns of turbidite elements and their well log responses, and the nature of sequence boundaries.

1.4 sequences (Figures 26 and 27). The geometries of these channel fills are not clear on the horizon slices, because of low seismic resolution and the complicated structures of these sequences. However, their general trends can be defined by high-amplitude anomalies, which trend the NE-SW direction (Figure 27). A root mean square (RMS) amplitude map of 1.9-2.4 Ma sequence shows a high-amplitude area (blue and pink color) trending NE-SW, which is consistent with the high amplitude distribution on the horizon slice and can be interpreted as a sand-prone depositional channel system. The coarse-grained channel fills incased in shale-prone overbank sediments are probably represented by the relatively high amplitude, because of their big impedance difference. Stelting et al. (1985) reported a similar example from the modern channel system. Well log responses of these channels show fining upward or blocky sand bodies. The coarsest sediment supplied into modern fans is generally located in channels themselves (Stelting et al., 1985).

Overbank deposits are generally fine-grained and thin-bedded turbidite sediments that can be laterally extensive and are adjacent to the main channels in a turbidite system. On seismic sections they show the seismic patterns consisted of low-amplitude, subparallel and moderate-to-fair coherence of reflectors. Well-log curves measured in overbank intervals are interpreted as shale-dominant sediments interbeded with thin sands or silt sediments. Figure 33 shows that a series of horizon slices of seismic facies A and B, in which overbank sediments were represented as low-amplitude areas deposited as unconfined flows filling the interchannel area. This channel, levee and overbank system is very well developed and well defined from both seismic section and horizon slices (Figure 27).

4.4.2 Erosional Channel Fills

Erosional channels are usually common in the upper slope, where the high downward slope accelerates the gravity flows (Galloway, 1998). In this study, only one erosional channel system (seismic facies E) was defined in the 0.8-0.7 Ma sequence where an erosional channel cut into the underlying sequence (Figure 28). During the

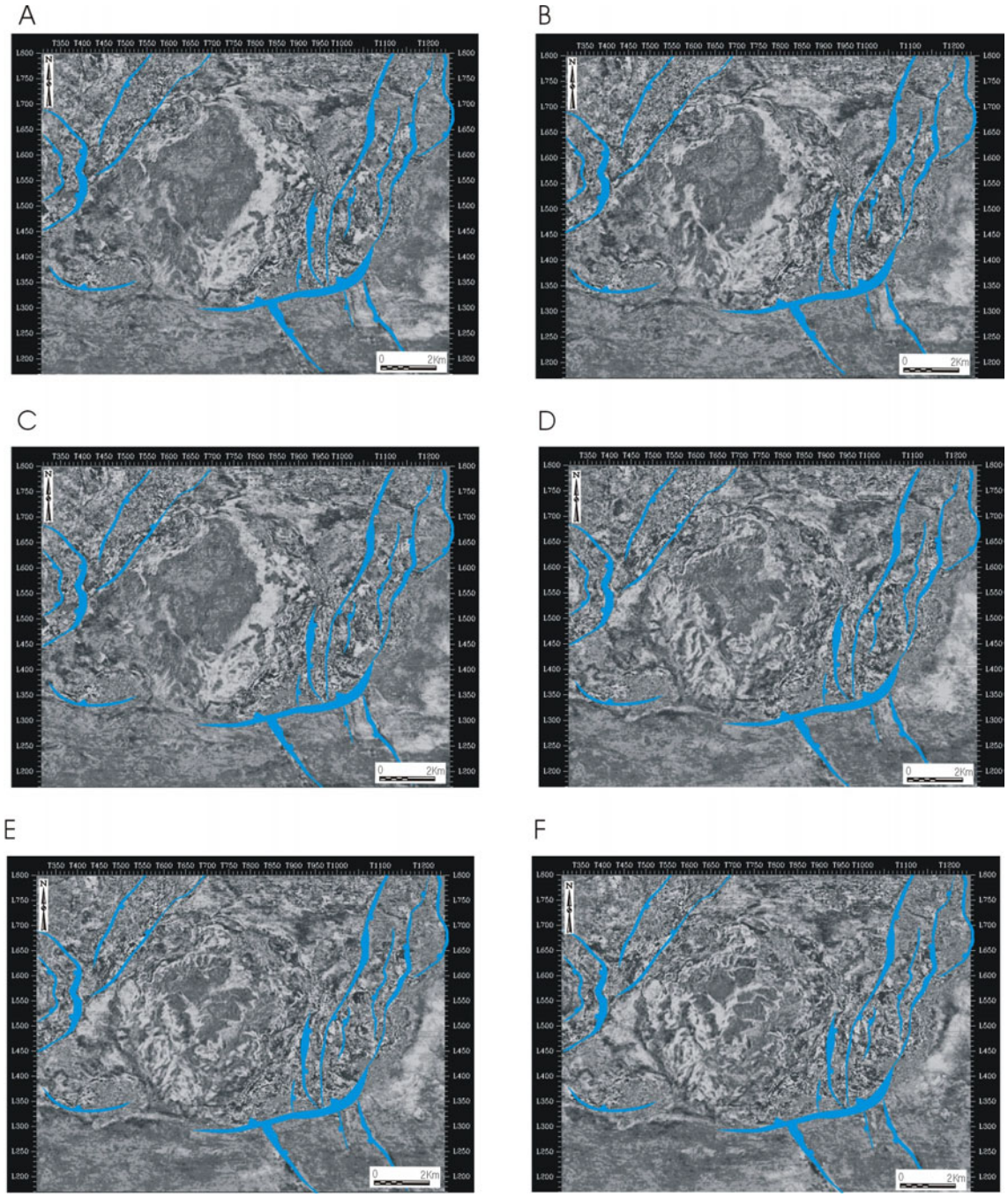

Figure 33. Horizontal seismic slices showing depositional channel and overbank facies of 0.7-0.6 Ma sequence. Every slice was cut parallel with underlying 0.7 Ma sequence boundary. A: 76 msec above; B: 80 msec above; C: 84 msec above; D: 90 msec above; E: 94 msec above; F: 98 msec above. Shades of white indicate intensity of negative impedance and shades of black indicate intensity of positive impedance.

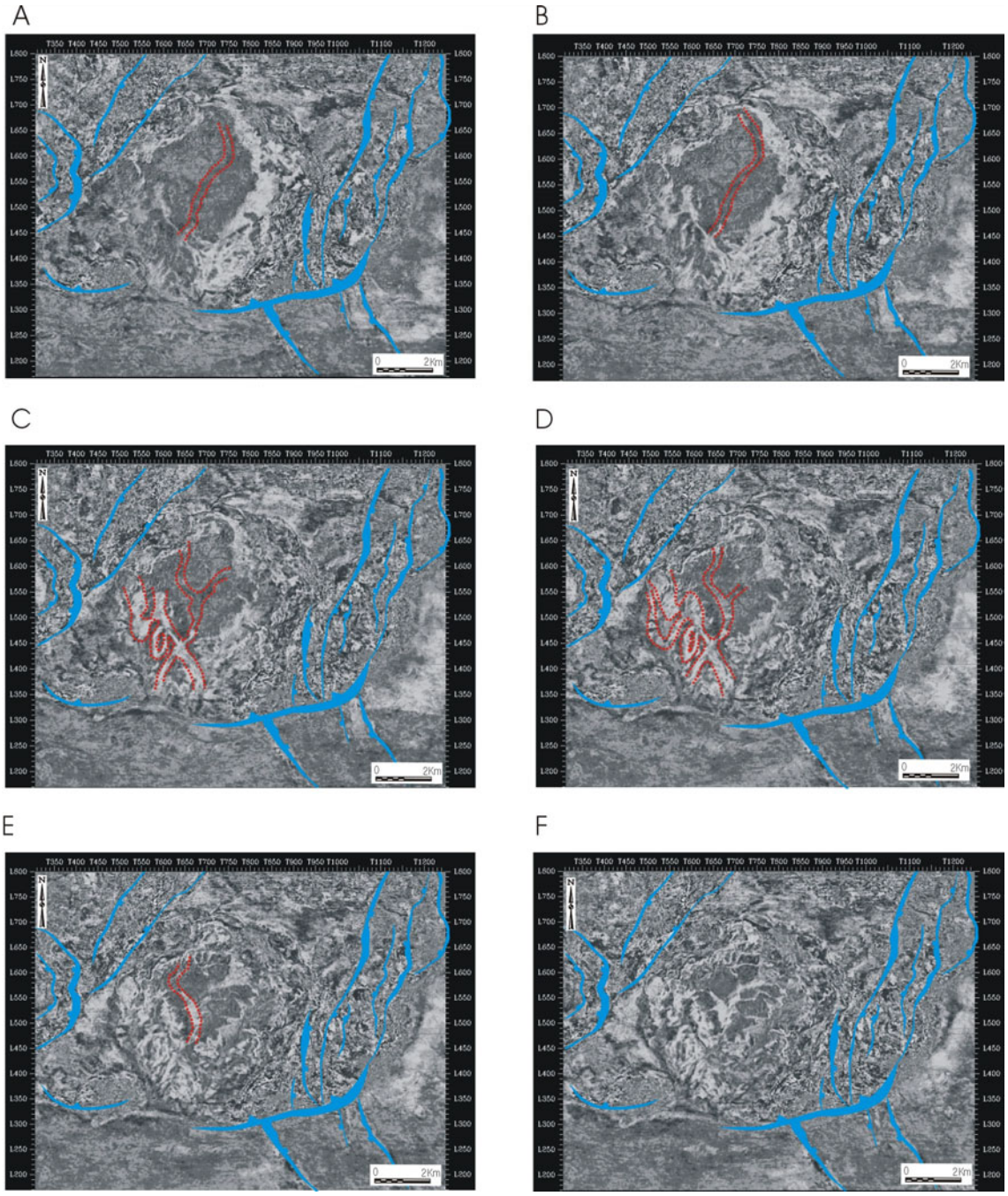

Figure 34. Series of horizontal slices as same as Figure 33 with channel interpretation.

early time of the lowstand stage, these channels might have been used as conduits to the downdip slope basin. The erosional channel is easily defined on the vertical seismic sections by its erosional features, but the horizon slice of these channels could not reveal the clear feature of these erosional channel fills (Figure 28), because the erosional channel was thought to be filled by shale dominant sediments and those shale-prone channel bodies could not be easily differentiated from the adjacent shale prone condensed sections. This facies trends a north-south direction with less sinuosity and greater width than depositional channels.

4.4.3 Mud Turbidite Fills and Sheets

This turbidite element is interpreted to fill and deposits in slope depressions, and it frequently laps out against bathymetric highs. Well-log responses for this element show that it is mud-dominant facies, but may be serrated if interbedded by silt/sand. Figure 29 shows the horizon slice that was cut parallel to the 1.4 Ma sequence boundary at 56 msec above the 1.4 Ma sequence boundary. It cut seismic facies D (Figure 23 and 24) and shows widely deposited, low-amplitude, high-coherency seismic characteristics without significant variation.

4.4.4 Pelagic and Hemipelagic Drapes

Hemipelagic and pelagic sediments typically drape the slope and adjacent basin floor. On the slope, suspended sediments play a major role during transgression and highstand in relative sea level. Where sediment accumulation rates are low, hemipelagic and pelagic sediments will be deposited (Stanley, 1985). Hemipelagic deposits thus form condensed sections with high radioactivity and high organic content. Seismic facies E is interpreted as hemipelagic and pelagic drapes. The characteristics of seismic facies E, characterized by high amplitude reflectors without significant amplitude variation covering all of the study area, indicate that this facies is deposited very widely, covering the previous topography with consistent thickness throughout the basin (Figures 22 and

23). In horizon slices, this facies shows a very widely deposited high-amplitude area with good coherency (Figure 30). Most of the sequences were topped by hemipelagic facies that were deposited during the late stage of the lowstand, transgression and highstand systems tracts (Figure 32 and 34). This sediment was deposited during most of the time span of one sea-level cycle, but is represented as thin and mud-dominant sediments. These sediments are well identified from seismic data that are characterized by strong, continuous reflectors with consistent thickness. From the well logs, this facies is well-distinguished by higher gamma ray values from the other mud dominant facies, and its thickness was usually less than 100 ft in the study area.

4.4.5 Turbidite Lobes

In deep-water settings, turbidite lobes are the most frequently drilled reservoir facies (Sangree et al., 1990) that are usually deposited directly on the lower sequence boundary. Turbidite lobes are spatially localized accumulations of sandy dominant sediments. Stacked deposits of coarse-grained turbidite form mounded lobes that have relatively restricted aerial distribution. In this study, one-turbidite lobe was interpreted in the 1.1 – 0.8 Ma sequence. In seismic data the turbidite lobe was shown as the mound shape seismic reflections with high amplitude and high coherency of seismic reflectors, downlapping onto the underlying sequence boundary (Seismic facies F). In terms of seismic patterns, this lobe is similar to hemipelagic drapes. However, hemipelagic drapes show almost constant thickness throughout the basin and show no lapout features, while turbidite lobes show mound-shape geometry, downlapping onto the underlying sequence boundaries. In horizon slices, this lapout feature might be observed as a changing amplitude and coherency. However, to the north and west, its lapout patterns are not clear. This lobe also shows a phase change in the horizon slice because it thins toward eastward. No wells were penetrated in the thick part of this facies where sand-prone sediments are expected. Several wells were drilled only in the marginal parts of this facies where the shapes of the logs show mud-prone sediment or serrated log patterns.

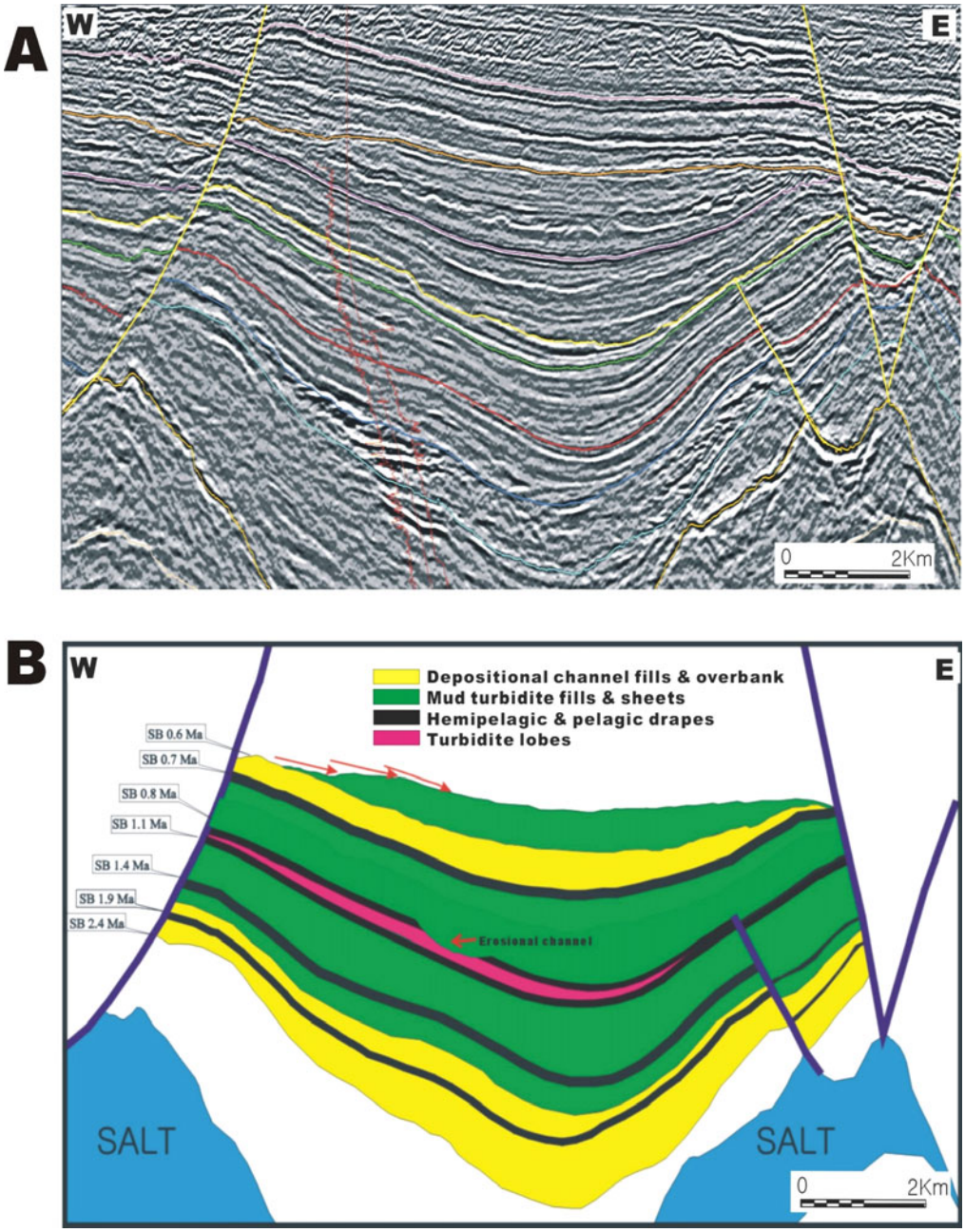

Figure 35. Vertical stacking patterns of turbidite elements from 2.4 Ma to 0.6 Ma sequence boundaries. A: depositional strike-oriented seismic section. B: turbidite element interpretation based on well logs and seismic facies. See Figure 4 for the location of section.

4.5 Facies Descriptions of Sequences

A depositional sequence in deep water is usually composed of basin floor fans (turbidite lobes), slope fans and condensed sections (Yielding, 1994). However, no sequences interpreted from this study show the complete succession of these three systems tracts. Especially, the turbidite lobe was very rare and was identified for only one sequence (1.1-0.8 Ma). According to Weimer et al. (1998), basin floor fans (turbidite lobes) tend to occur more commonly in lower slopes and older sequences (Weimer et al., 1998). Therefore, it is inferred that the study area located in the middle-to-upper slope during the deposition of these sequences was not a favorable condition for turbidite-lobe deposition. Slope fans are the dominant systems tracts in the study area, which can be subdivided into three turbidite elements: depositional channel fills and overbank, mud turbidite fills and sheets, and erosional channel fill. Sand-prone depositional channel fills and turbidite lobes mainly occurred in the lower parts of sequences, while mud-turbidite fills and sheets and hemipelagic and pelagic drapes were dominantly deposited in the upper parts of sequences. Overall, each sequence shows fining-upward patterns and the older sequences are more sand-prone than the younger ones (Figures 33 and 34).

4.5.1 2.4-1.9 Ma Sequence

The 2.4-1.9 Ma sequence consists of channel fill and overbank deposits and overlying condensed intervals. Well logs indicate that this is one of the most sand-prone sequences in the study area (Figure 19). In seismic, this channel system is represented as a bi-directional-downlapping mound shape with high amplitude and low coherency. Well logs are represented as fining upward (bell shape) or blocky patterns indicating a complex amalgamated channels with thickness measured up to about 30 ft in Well 358-1 (Figure 18). These sand-prone channel-fill sediments are adjacent to overbank sediments that are characterized by low amplitude, high coherency and parallel to subparallel seismic reflections. Horizon slices generated by sequence boundary 1.9 Ma

show the general trend of this channel system, in which the depositional channel facies are located in northwestern part of the basin trending northeast to southwest (Figure 25). However, the exact channel geometry was not defined from the horizon slices because of the limited seismic resolution and structural complexity caused by fault and salt deformation. The general external shape of this sequence is interpreted as trough fills thinning to the east and west of salt highs. The depocenter of the sequence is located in the central part of the basin trending northeast to southwest, which is generally compatible with depositional channel systems interpreted from the horizon slices (Figure 10 and 26). The thickest sedimentation occurred in the downdip area of this basin. The abnormal isochron area located line 350, trace between 300 and 600 in Figure 10-A is not real, great thickness of which was caused by sediment overlap in reverse faults. The upper and lower sequence boundaries were partly eroded by overlying channels. Where erosion occurred, no condensed sections were observed (as in Wells 350-2 and 351-1: Figure 32 and 35).

4.5.2 1.9-1.4 Ma Sequence

The 1.9-1.4 Ma sequence is composed of depositional channel fills and overbank deposits, mud turbidite fills and sheets, and condensed intervals (Figure 32 and 35). The depositional channel fills are thin and the channels are small comparing with the depositional channels in underlying sequence. In Well 358-1, well data shows about a 200-ft fining-upward sand, which is interpreted as an amalgamated channel-fill deposit. However, the gamma ray curve shows no difference from the shale strata underlying. This suggests that this sand body contains some radioactive minerals resulting its high gamma ray values. From the horizon slice, one channel system trending in NNE-SSW direction was defined. This channel system is characterized by negative high amplitude, which is interpreted as a channel sands incased in overbank shale.

Mud turbidite fills and sheets overlying depositional channels are represented by thick shale interval, interbedded occasionally with hemipelagic shale and thin sand bodies. This sediment can be differentiated from condensed sections consisting of

hemipelagic and pelagic drapes, because condensed intervals have higher gamma ray values and higher amplitude and coherency than this facies. A couple hemipelagic and pelagic intervals are defined for this sequence based on well data and biostratigraphic information (Figure 32 and 35). However, only one condensed interval was defined in the updip area of the basin (Well 350-1, 350-2). A condensed interval occurring between two mud turbidite fill sediments is not a major condensed section. It is interpreted that it was deposited during lowstand in relative sea level by sediment starvation probably caused by channel avulsion. The isochron map shows the depocenter of this sequence was located in the central part of the basin trending northeast to southwest (figure 10 B), which is very conformable with the depositional channel system developed in this sequence (Figure 10 and 27). The upper sequence boundary is in general conformable with the overlying mud turbidite fills and sheets, and the condensed interval underlying the sequence boundary is well preserved for this sequence.

4.5.3 1.4-1.1 Ma Sequence

The 1.4-1.1 Ma sequence is characterized by the highest sedimentation rate in the study area. All the sediment deposited during this time is mud-prone: mud turbidite fills and condensed intervals. Well data show very thick mud-dominant sediment intercalated with thin sand and silt intervals. In the seismic sections, mud turbidite fills are parallel-to-subparallel, fair-to-low amplitude seismic reflectors. Horizon slices show laterally homogenous low amplitude patterns without abrupt changes throughout the study area. This facies is very broadly deposited and filled the basin with mud-dominant sediment as unconfined flows.

The sediment bodies are commonly thinning against salt-high areas. Some reflectors onlap underlying reflectors. According to the isochron map of this sequence, there are two depocenters; one is located in the northern part of the basin and the other is in the southeastern part of the basin. The one in the northern part of the basin was developed by listric normal fault that provided additional accommodation during the deposition of this sequence (Figure 7). Well-log responses measured in this interval

indicate mud prone sedimentation with thin sand or silt intercalations. Two hemipelagic and pelagic facies were defined from this sequence. These condensed intervals are well represented in seismic and well data. In seismic data, they are characterized by strong continuous reflectors with consistent thickness throughout the basin, indicating that they were mainly composed of pelagic and hemipelagic suspended sediments. In well data these facies were distinguished from mud turbidite fill sediments by their gamma ray values that are higher than those of mud-turbidite fills. The sequence boundaries on top and bottom are conformable with other sequences.

4.5.4 1.1-0.8 Ma Sequence

This sequence is characterized by very slow sedimentation indicated by its isochron map, in which the maximum thickness is less than 120 msec in two-way times, which might be explained by sediment starvation in this area caused by channel avulsion. However, no further information was available for this study. This sequence consists of turbidite lobes and hemipelagic and pelagic sediments. A turbidite lobe is characterized by high-amplitude, high-coherency, mound-shape reflectors that can be interpreted as sand-prone turbidite lobe, deposited in the early stage of lowstand systems tracts and hemipelagic and pelagic sediments were deposited until the next lowstand in sea level. No significant Mud turbidite fills and sheets and depositional channel fills and overbank deposits were deposited for this sequence. The isochron map shows that the thickness of this sequence decreases toward east, which can be explained by the thickness change of turbidite lobe. In plan view turbidite lobe is an elliptical shape, thinning to the east, which caused the amplitude phase change from west to east on horizon slice (Figure 28). The sedimentation of this sequence was also controlled by listric faults in the northern part of the basin where a small scale depocenter was formed. The upper sequence boundary was partly eroded by erosional channel that was developed in the early stage of lowstand systems tract and eroded out the underlain hemipelagic and pelagic drapes.

4.5.5 0.8-0.7 Ma Sequence

The 0.8-0.7 Ma sequence is composed of erosional channel fills, mud turbidite fills and sheets, and an overlying condensed interval. These channels, down-cutting the underlying sequence, are elongated in the north-south direction and filled by mud-dominant channel abandonment sediments. These channels are very wide compared with other depositional channels observed in the study area. This erosional channel developed in the early stage of the lowstand in relative sea level that transported sediment to downslope area and then was filled by mud-dominant sediments. This channel is not clearly defined on the horizon slices even though it is clear in vertical sections. It is because it was filled by mud-prone sediment, of which acoustic impedance is similar with the underlying sediments. Using vertical seismic sections, these channels were mapped on the horizon slices, by which they are represented as a relatively low-amplitude area surrounded by a high-amplitude area of the condensed sections. An isochron map shows an elliptical shape depocenter in the central part of the basin, indicating that sedimentation was mainly controlled by salt withdrawal activity. The time thickness of this sequence ranges from 350–120 msec in the basin area. The upper sequence boundary is conformable with the sequence above.

4.5.6 0.7-0.6 Ma Sequence

The 0.7-0.6 Ma sequence consists of depositional channel fills, overbank deposits and mud turbidite fills. No condensed sections were observed from this sequence (Figures 33 and 34). It is interpreted that the condensed section that had deposited in the upper part of this sequence was eroded out by the bypass sediment during the early stage of next sequence. The 0.6 Ma sequence boundary is the most predominant erosional surface in this area. Less sediment was eroded in the central part of the basin because of the accelerated subsidence by salt withdrawal in this area, in which part of mud-turbidite sediments were preserved, but in the northern and southern parts, only channel levee systems were preserved.

The depositional channel fills and overbank deposits are very well preserved and easily defined from vertical seismic sections and horizon slices. A series of horizon slices show that there were two channel systems trending northeast to southwest and northwest to southeast (Figure 33 and 34). These channels are highly sinuous with good levee systems, which are characteristic of a low-gradient, mud-dominant depositional slope (Clark et al., 1992). No well data were available for these channel-fill sediments. However, their seismic characters represented by sinuous high-amplitude areas are interpreted as sand-prone deposits. The time thickness of this sequence ranges from 320 msec at the central part of the basin to less than 100 msec near the salt-high areas that was mainly controlled by salt withdrawal from the basin.

5. CONCLUSION

During the Late Pliocene to Early Pleistocene, sediments deposited in the study area were mainly transported by gravity flows and deposited in an intraslope salt-withdrawal basin. This basin is an elliptical shape, trending to the NNE-SSW direction. To the north, east and west the basin is bounded by extensional faults and shallow salt highs and to the south by salt-cored folds and reverse faults. These topographic highs functioned as partial downdip barriers to sedimentation, trapping more sediments within the basin. After 0.6 Ma, salt evacuated from the central part of the basin, which was observed by a series of isochron maps, and resulted in infilling the salt-withdrawal basin. Even though this basin was severely deformed by salt and fault evolution, 3-D high-resolution seismic data could reveal the structural patterns of the study area.

Crossplot method of wireline logs combined with biostratigraphical data proves to be beneficial tool to define condensed intervals. Sequence boundaries were mainly lying above the condensed sections. Sequence stratigraphic analysis of well logs, biostratigraphic data and 3-D seismic data provided a chronostratigraphic framework of the study area, through which seven sequence boundaries were identified. Most sequence boundaries are in general conformaties, but 1.9 Ma, 0.8 Ma and 0.6 Ma sequence boundaries were interpreted as partially or fully eroded surfaces caused by submarine channels or bypass sediments such like debris flows, slump and slide.

Seismic reflection characteristics including amplitude, coherency of reflectors, and reflection configuration were examined and each sequence was subdivided into separate seismic facies. Seismic volumes flattened by reference horizons revealed the lateral variations of these facies. They are useful in describing the spatially confined facies, especially for channel-like features. Seismic facies descriptions from vertical seismic sections and horizon slices were combined with well data and interpreted into turbidite elements. Five turbidite elements were defined: (1) depositional channel fills and

overbank deposits, (2) erosional channel fills, (3) mud turbidite fills and sheets, (4) turbidite lobes, and (5) hemipelagic and pelagic drapes.

Depositional channel fills are the most common sand-prone facies in the study area. They are usually deposited in the lower part of depositional sequence. Well logs measured for these facies show bell-type or cylinder-type log patterns indicating sand-prone facies. The lateral variations of these sand-prone channels were revealed by horizon slices, in which they are characterized by elongated sinuous, high amplitude area surrounded by broad low amplitude area. Overbank deposits are generally fine-grained turbidite sediments that can be laterally extensive and are adjacent to the depositional channels. Turbidite lobe is interpreted as the sand-dominant facies in slope basin. Only one turbidite lobe was interpreted in the 1.1 – 0.8 Ma sequence, which shows high amplitude and continuous reflections with the mound shape, downlapping onto the underlying sequence boundary. In horizon slices, this lapout feature might be observed as a changing amplitude and coherency. No wells were penetrated in the thick part of this facies where sand-prone sediments are expected. Erosional channel fills were defined only in the 0.8-0.7 Ma sequence where erosional channel cut into the underlying sequence, functioned as conduits to the downdip slope basin. This erosional channel was filled by low amplitude, moderate coherence of subparallel reflections, interpreted as mud-prone sediments. Mud turbidite fills and sheets are interpreted to have filled in slope depressions mainly as unconfined flows. Well-log responses for these intervals show that they are mud-dominant facies, but may be serrated if interstratified by silt/sand. In plan view, they show low-amplitude, high-coherency seismic characteristics without significant variation. Hemipelagic and pelagic sediments typically drape widely the slope and adjacent basin floor and represented by strong continuous reflections in vertical sections and horizon slices. It can be distinguished by its consistent thickness from turbidite lobes.

Depositional sequences in the study area usually consist of depositional channel fills and overbank deposits, mud turbidite fills and sheets, and hemipelagic and pelagic drapes. Sand-prone depositional channel fills and turbidite lobes mainly occurred in the

lower parts of sequences, while mud-turbidite fills and sheets and hemipelagic and pelagic sediments were dominantly deposited in the upper parts of sequences. Overall, each sequence shows fining-upward patterns topped by hemipelagic and pelagic drapes. It is also clear the older sequences are more sand-prone than the younger sequences.

The geometries of sand-prone turbidite facies were described by seismic facies analysis with high-resolution 3-D seismic data, which was performed within a sequence stratigraphic framework. Horizon slices cut parallel with sequence boundaries or condensed sections could reveal the lateral variations of the spatially confined reservoir facies, but their applications were limited by the seismic qualities, structural complexities and the vertical seismic resolutions. Seismic facies analysis with 3-D seismic combined with horizon slices made it possible to describe the geometries of turbidite elements in three dimensions, which will be used to predict the distributions of reservoir, seal, and source facies in intra-slope basins and to locate stratigraphical traps in deep water basins.

REFERENCES CITED

Bouma, A. H., H. H. Roberts, and J. M. Coleman, 1990, Acoustical and geological characteristics of near-surface sediments, upper continental slope of northern gulf of Mexico: Geo-Marine Letters, v. 10, p. 200-208.

Brown, L. F., and W. L. Fisher, 1977, Seismic-stratigraphic interpretation of depositional systems: examples from Brazil rift and pull-apart basins, *in* C. E. Payton, ed., Seismic stratigraphy: applications to hydrocarbon exploration: AAPG Memoir 26, p. 213-248.

Clark, J. D., N. H. Kenyon, and K.T. Pickering, 1992, Quantitative analysis of the geometry of submarine fans: Geology, v. 20, p. 633-636.

Galloway, W. E., 1998, Siliciclastic slope and base-of-slope depositional systems: Component facies, stratigraphic architecture, and classification: AAPG Bulletin, v. 82, no. 4, p. 569-595.

Geitgey, J. E., 1998, Plio-Pleistocene evolution of central offshore Louisiana: Gulf Coast Association of Geological Societies Transactions, v. 38, p. 151-156.

Haq, B. U., 1991, Sequence stratigraphy, sea-level change, and significance for the deep sea, *in* D. I. M. Macdonald, ed., Sedimentation, tectonics and eustacy: sea-level changes at active margins: Society of Economic Paleontologists and Mineralogists Special Publication 12, p. 3-39.

Haq, B. U., J. Hardenbol, and P. R. Vail, 1988, Mesozoic and Cenozoic chronostratigraphy and cycles of sea-level change, *in* C. K. Wilgus, B. S. Hastings, C. G. St. C. Kendall, H. W. Posamentier, C. A. Ross, J. C. Van Wagoner, eds., Sea-level changes: an integrated approach: Society of Economic Paleontologists and Mineralogists Special Publication 42, p. 71-108.

Mitchum, R.M., and J. C. Van Wagoner, 1991, High-frequency sequences and their stacking patterns: sequence-stratigraphic evidences of high-frequency eustatic cycles: Sedimentary Geology, v. 70, p. 131-160.

Mitchum, R. M., Jr., P. R. Vail, and S. Thompson, 1977, Seismic stratigraphy and global changes of sea level, part 2: the depositional sequence as a basic unit for stratigraphic analysis, *in* C. W. Payton, ed., Seismic stratigraphic applications to hydrocarbon exploration: AAPG Memoir 26, p. 53-62.

Mitchum, R. M., J. B. Sangree, P. R. Vail, and W. W. Wornardt, 1990, Sequence stratigraphy in Late Cenozoic expanded sections, Gulf of Mexico, *in* J. M. Armentrout and B. F. Perkins, eds., Sequence stratigraphy as an exploration tool, concepts and practices in the Gulf Coast: Gulf Coast Section, SEPM Foundation, Eleventh Annual Research Conference, Houston, Texas, p. 237-256.

Morton, R. A., 1993, Attributes and origins of ancient submarine slides and filled embayments: examples from the Gulf Coast Basin: AAPG Bulletin, v. 77, no. 6, p. 1064-1081.

Mutti, E., and W. R. Normark, 1991, An integrated approach to the study of turbidite systems, *in* P. Weimer and M. H. Link, eds., Seismic facies and sedimentary processes of submarine fans and turbidite systems: New York, Springer-Verlag, p. 75-106.

Normark, W. R., 1978, Fan valleys, channels, and depositional lobes on modern submarine fans: characters for recognition of sandy turbidite environments: AAPG Bulletin v. 62, n. 6, p. 912-931.

Pacht, J. A., B. E. Bowen, B. L. Shaffer, and B. R. Pottorf, 1990, Sequence stratigraphy of Plio-Pleistocene strata in the offshore Louisiana Gulf Coast: applications to hydrocarbon exploration, *in* J. M. Armentrout and B. F. Perkins, eds., Sequence stratigraphy as an exploration tool, concepts and practices in the Gulf Coast: Gulf Coast Section, SEPM Foundation, Eleventh Annual Research Conference, Houston, Texas, p. 269-285.

Pirrie, D., 1998, Interpreting the record: facies analysis: *in* P. Doyle, and M. R. Bennett, eds., Unlocking the stratigraphic record: School of earth and environmental sciences, University of Greenwich, UK, p. 395-420.

Rider, M., 1995, The Geologic Interpretation of Well Logs, Gulf Publishing Company, London, 280 p.

Rowan, G. M., and P. Weimer, 1998, Salt-sediment interaction, Northern Green Canyon and Ewing Bank (Offshore Louisiana), Northern Gulf of Mexico: AAPG Bulletin, v. 82, no. 5B, p. 1055-1082.

Rowan, M. G., M. P. A. Jackson, and B. D. Trudgill, 1999, Salt-related fault families and fault welds in the Northern Gulf of Mexico: AAPG Bulletin, v. 83, no. 9, p. 1454-1484.

Sangree, J. B., P. R. Vail, and R. M. Mitchum, Jr., 1990, A summary of exploration applications of sequence stratigraphy, *in* J. M. Armentrout and B. F. Perkins, eds., Sequence stratigraphy as an exploration tool, concepts and practices in the Gulf Coast: Gulf Coast Section, SEPM Foundation, Eleventh Annual Research Conference, Houston, Texas, p.321-327.

Shaffer, B. L., 1990, The nature and significance of condensed sections in Gulf Coast late Neogene sequence stratigraphy: Gulf Coast Association of Geological Societies Transactions, v. 40, p. 767-776

Simmons, G. R., W. R. Bryant, R. Buffler, G. Lee, and C Fiduk, 1996, Regional distribution of salt and basin architecture in the northwestern Gulf of Mexico: *in* J. O. Jones and T. L. Freed, eds., A structural framework of the Northern Gulf of Mexico: A special publication of Gulf Coast Association of Geological Societies, p. 93-94

Stanley, D. J., 1985, Mud redepositional processes as a major influence on Mediterranean margin-basin sedimentation, *in* D. J. Stanley and F. C. Wezel, eds., Geological evolution of the Mediterranean Basin: New York, Springer-Verlag, p. 377-412.

Stelting, C. E., and DSDP Leg 96 Shipboad Scientist, 1985, Migratory characteristics of a mid-fan meander belt, Mississippi Fan, *in* A. H. Bouma, W. R. Normark, and N. E. Barnes, eds., Submarine fans and related turbidite systems: New York, Springer-Verlag, p. 283-290.

Vail, P. R., 1987, Seismic stratigraphy interpretation using sequence stratigraphy, Part I: seismic stratigraphy interpretation procedure *in* A. W. Bally, ed., Atlas of seismic stratigraphy: AAPG studies in Geology 27, p. 1-10.

Vail, P. R. and W. W. Wornardt, 1990, Well log-seismic sequence stratigraphy: an integrated tool for the 90s: *in* J. M. Armentrout and B. F. Perkins, eds., Sequence stratigraphy as an exploration tool, concepts and practices in the Gulf Coast: Gulf Coast Section, SEPM Foundation, Eleventh Annual Research Conference, Houston, Texas, p. 379-388.

Vail, P. R. and W. W. Wornardt, 1991, An integrated approach to exploration and development in the 90 sequence: well log-seismic sequence stratigraphy analysis: Gulf Coast Association of Geological Societies Transactions, v. 41, p. 630-650.

Van Wagoner, J. C., H. W. Posamentier, R. M. Mitchum, Jr., P. R. Vail, J. F. Sarg, T. S. Loutit, and J. Hardenbol, 1988, An overview of the fundamentals of sequence stratigraphy and key definitions, *in* C. K. Wilgus, B. S. Hastings, C. G. St. C. Kendall, H. W. Posamentier, C. A. Ross, J. C. Van Wagoner, eds., Sea-level changes: an integrated approach: Society of Economic Paleontologists and Mineralogists Special Publication 42, p. 39-46.

Van Wagoner, J. C., R. M. Mitchum, Jr., K. M. Campion, and V. D. Rahmanian, 1990, Siliciclastics sequence stratigraphy in well logs, cores, and outcrops: concepts for high-resolution correlation of time and facies: AAPG Methods in Exploration Series, no. 7, 55 p.

Varnai, P., 1998, Three-dimensional seismic stratigraphic expression of Pliocene-Pleistocene turbidite systems, northern Green Canyon, offshore Louisiana, northern Gulf of Mexico: AAPG Bulletin, v. 82, no. 5B, p. 986-1012.

Villamil, T., C. Arango, P. Weimer, A. Waterman, M. G. Rowan, P. Varnai, A. J. Pulham, and J. R. Crews, 1998, Biostratigraphic condensation, and key surface identification, Pliocene and Pleistocene sediments, northern Green Canyon and Ewing Bank (offshore Louisiana), northern Gulf of Mexico: AAPG Bulletin, v. 82, no. 5B, p. 961-985.

Wagner, J. B., Morin, R. W., Ford, D. W., Mathur, V. R., and Mauro, R. T., 1994, A sequence stratigraphic analysis of the Lower Miocene, West and East Cameron areas, Gulf of Mexico: preliminary results, *in* P. Weimer, A. H. Bouma, and B. F. Perkins, eds., Submarine fans and turbidite systems: Gulf Coast Section, SEPM Foundation, Fifteenth Annual Research Conference, Houston, Texas, p. 357-372.

Walker, R. G., 1992, Turbidites and submarine fans, *in* R. G. Walkers and N. P. James eds., Facies models: response to sea level change: Geological Association of Canada, p. 239-263.

Watkins, J. S., J. Xi, R. Li, S. Huh, J. Zhang, and F. Xue, 1996, Depocenter formation and distribution on the Texas and Louisiana Shelves, Gulf of Mexico: *in* J. O. Jones and T. L. Freed, eds., A structural framework of the Northern Gulf of Mexico: A special publication of Gulf Coast Association of Geological Societies, p. 99-101

Weimer, P., P. Varnai, A. Navarro, Z. Acosta, F. Budhijanto, R. Martinez, M. G. Rowan, B. McBride, and T. Villamil, 1994, Sequence stratigraphy of Neogene turbidite systems, Green Canyon and Ewing Bank, northern Gulf of Mexico: preliminary results, *in* P. Weimer, A. H. Bouma, and B. F. Perkins, eds., Submarine fans and turbidite systems: Gulf Coast Section, SEPM Foundation, Fifteenth Annual Research Conference, Houston, Texas, p. 383-399.

Weimer, P., P. Varnai, F. M. Budhijanto, Z. M. Acosta, R. E. Martinez, A. F. Navarro, M. G. rowan, B. C. McBride, T. Villamil, C. Arango, J. R. Crews, and A. J. Pulham, 1998, Sequence stratigraphy of Pliocene and Pleistocene turbidite systems, northern Green Canyon and Ewing Bank (offshore Louisiana), northern Gulf of Mexico: AAPG Bulletin, v. 82, no. 5B, p. 918-960.

Winker, C. D., 1984, Clastic shelf margins of the Post-Comanchean Gulf of Mexico: Implications for deep-water sedimentation, *in* D. G. Bebout, and E. A. Mancini, eds., Characteristics of Gulf Basin deep-water sediments and their exploration potential: Gulf Coast Section, SEPM Foundation, Fifth Annual Research Conference, Dallas, Texas, p. 109-117.

Whittaker, A., 1998, Principles of seismic stratigraphy, *in* P. Doyle and M. R. Bennett, eds., Unlocking the stratigraphical record: Advances in modern stratigraphy: Chichester, UK, John Wiley and Sons, p. 275-298.

Yeilding, C. A., and G. M. Apps, 1994, Spatial and temporal variations in the facies associations of depositional sequences on the slope: Examples from the Miocene-Pleistocene of the Gulf of Mexico: preliminary results, *in* P. Weimer, A. H. Bouma, and B. F. Perkins, eds., Submarine fans and turbidite systems: SEPM Gulf Coast Section Fifteenth Annual Research Foundation Conference, p. 425-437.

VITA

Booyong Kim
1588-14 Kwanyang-Dong, Dongan-Gu,
Kyungki-Do, 431-711
South Korea
E-mail: booyong@knoc.co.kr

Booyong Kim received his B.S. in geology from Kyungpook National University in February 1992. After graduation, he joined the Korea National Oil Corporation (KNOC) on May 1, 1993 and worked as an exploration geologist in the Domestic exploration area. In August, 1997 he entered Texas A&M University pursuing a M.S. in Geophysics. After two years, he returned to KNOC and has been working on Korean offshore projects. He received his M.S. in geophysics in August 2002.